Fall 1994

Low pressure chemical vapor deposition of silicon nitride films from ditertiarybutylsilane

Xiangqun Fan
New Jersey Institute of Technology

Copyright Warning & Restrictions

The copyright law of the United States (Title 17, United States Code) governs the making of photocopies or other reproductions of copyrighted material.

Under certain conditions specified in the law, libraries and archives are authorized to furnish a photocopy or other reproduction. One of these specified conditions is that the photocopy or reproduction is not to be "used for any purpose other than private study, scholarship, or research." If a, user makes a request for, or later uses, a photocopy or reproduction for purposes in excess of "fair use" that user may be liable for copyright infringement,

This institution reserves the right to refuse to accept a copying order if, in its judgment, fulfillment of the order would involve violation of copyright law.

Please Note: The author retains the copyright while the New Jersey Institute of Technology reserves the right to distribute this thesis or dissertation

Printing note: If you do not wish to print this page, then select "Pages from: first page # to: last page #" on the print dialog screen

ABSTRACT

LOW PRESSURE CHEMICAL VAPOR DEPOSITION OF SILICON NITRIDE FILMS FROM DITERTIARYBUTYLSILANE

by
Xiangqun Fan

In this study amorphous stoichiometric silicon nitride films were synthesized by low pressure chemical vapor deposition (LPCVD) using DTBS (ditertiarybutylsilane) and ammonia (NH_3). The growth kinetics were determined as a function of temperature in the range of 600-900 $^{\circ}C$, pressure in the range of 0.2-1.1 Torr, DTBS flow rate in the range of 10-50 sccm, and NH_3/DTBS flow ratio in the range of 5-20. At constant condition of pressure (0.5 Torr), DTBS flow rate (10sccm) and NH_3 flow rate (100 sccm), the deposition rate of as-deposited silicon nitride films was found to follow an Arrehnius behavior in the temperature range of 600-700 $^{\circ}C$ with an activation energy of 50.0±0.2 kcal mol^{-1}. The film characterizations including physical, compositional, structural, optical and mechanical properties were determined by using Nanospec Interferometry, XPS, RBS, X-ray diffraction, FTIR, UV Visible, Ellipsometer, and Nano Instrument Indenter. The obtained results demonstrated the feasibility of using DTBS in the synthesis of high quality silicon nitride films by LPCVD. Furthermore, some advantages of DTBS over traditional precursors were found and thus indicated that high quality amorphous silicon nitride films can be obtained from DTBS-NH_3 precursor system using LPCVD by optimizing the film synthesis conditions.

LOW PRESSURE CHEMICAL VAPOR DEPOSITION OF SILICON NITRIDE FILMS FROM DITERTIARYBUTYLSILANE

by
Xiangqun Fan

A Thesis
Submitted to the Faculty of
New Jersey Institute of Technology
in Partial Fulfillment of the Requirements for the Degree of
Master of Science in Engineering Science

Interdicipplinary Program in Materials Science and Engineering

October 1994

APPROVAL PAGE

LOW PRESSURE CHEMICAL VAPOR DEPOSITION OF SILICON NITRIDE FILMS FROM DITERTIARYBUTYLSILANE

Xiangqun Fan

Dr. Roland A. Levy, Thesis Advisor — Date
Professor of Physics,
Director of Materials Science and Engineering Program, NJIT

Dr. James M. Grow, Thesis Advisor — Date
Professor of Chemical Engineering, Chemistry, and
Environmental Science, NJIT

Dr. David Kristol — Date
Professor of Chemistry,
Director of Biomedical Engineering Program, NJIT

BIOGRAPHICAL SKETCH

Author: Xiangqun Fan

Degree: Master of Science in Engineering Science

Date: October 1994

Undergraduate and Graduate Education:

- Master of Science in Engineering Science,
  New Jersey Institute of Technology,
  Newark, New Jersey, May 1994
- Bachelor of Science in Semiconductor Materials,
  Shanghai University of Science and Technology
  Shanghai, P.R.China, July 1986

Major: Materials Science and Engineering

Professional Background

- Research Associate,
  Shanghai Institute of Metallurgy, Chinese Academy
  July 1986 - December 1993

This thesis is dedicated to
my parents, Biyun Shu and Maozhong Fan

ACKNOWLEDGMENT

The author wishes to express her sincere gratitude to her advisors, Professor Roland A. Levy and James M. Grow, for their guidance, friendship, moral and financial support throughout this thesis work, without which it would not have been completed.

Special thanks to Professor David Kristol for serving as member of the committee.

The author appreciates the timely help and suggestions from the CVD Laboratory members, including: Vitaly Sigal, Bozena Szkudlarski, Venkat Paturi, Mahalingam Bhaskaran, Wei-Ching Liang, Shingo Uto, Wei-shang King, Yan Gao, Xin Lin, and Abhijit Datta.

TABLE OF CONTENTS

Chapter Page

Chapter Page

LIST OF TABLES

LIST OF FIGURES

Figure Page

CHAPTER 1

INTRODUCTION

Silicon nitride is a hard, chemically inert, dielectric material which forms an excellent diffusion barrier to H_2O, Na and many other ionic species [1]. It is widely used in numerous semiconductor applications for insulation, isolation, passivation and etch masking.

There are many techniques available for synthesizing silicon nitride films [2], including chemical vapor deposition (CVD), chemical transport, direct nitridation [3], vacuum evaporation [4], and ion implantation [5]. CVD is preferred in semiconductor applications because of the excellent step coverage, uniformity, and high throughput that it provides [2].

CVD synthesis of silicon nitride films is currently based on the use of chlorosilanes as sources of silicon. These precursors are generally hazardous and highly corrosive. This study focuses on the use of an environmentally benign precursor, namely, ditertiarybutylsilane (DTBS) as an alternate source for silicon to synthesize amorphous silicon nitride films by low pressure chemical vapor deposition (LPCVD). The kinetics of deposition are investigated as a function of processing variables, and the interrelationships amongst these processing variables, resulting compositions, and properties are established. In this thesis, the fundamental aspects of CVD will first be covered, followed by a discussion of the properties and applications of silicon nitride films as well as a description of the experimental set-up and an analysis of the film characterization techniques used in this work. The experimental data will then be discussed and conclusions based on the results drawn.

1.1 Basic Aspects of Chemical Vapor Deposition

1.1.1 Principles and Mechanisms

A CVD process can be summarized as consisting of the following sequence of steps [6]:

a) A given composition (and flow rate) of reactant gases and diluent inert Gases is introduced into a reaction chamber.

b) the gaseous species diffuse to the substrate.

c) the reactants are adsorbed on the substrate.

d) the adsorbed reactants undergo migration and film forming chemical reactions.

e) the gaseous by-products of the reaction are desorbed.

f) gaseous transport of by-products.

g) bulk transport of by-products out of reaction chamber.

The energy required to drive the reactions can be supplied by several methods including heat, photons, and ions, with thermal energy being the most commonly used [7].

In practice, there are two kinds of chemical reactions leading to the formation of a solid material [8]. One is heterogeneous reaction that occurs on (or very close to) the wafer surface, the other is homogeneous reaction that takes place in the gas phase. Heterogeneous reactions are more desirable because they occur only on the heated substrate surface and can produce good quality films. Homogeneous reactions are generally undesirable because they form gas phase clusters which results in poor quality films. Thus, one important consideration in CVD is the degree by which heterogeneous reactions are favored over those generated in the gas phase.

Heterogeneous surface reactions involving one molecular of a reactant can be treated by Langmuir adsorption isotherm [9, 10]. Let θ be the fraction of

surface that is covered and (*1*-θ) the fraction that is bare. The rate of adsorption is then $k_1 p(1-\theta)$, where p is the gas pressure and k_1 is proportionality constant, the rate of desorption is $k_{-1}\theta$. At equilibrium, the rates of adsorption and desorption are equal, so that

$$\frac{\theta}{1-\theta} = \frac{k_1}{k_{-1}} p = Kp \tag{2.1}$$

where K, equal to k_1/k_{-1}, is the adsorption equilibrium constant. This equation can be written as

$$\theta = \frac{Kp}{1+Kp} \tag{2.2}$$

The rate of reaction is proportional to θ and may therefore be written as

$$D.R. = k_2\theta = \frac{k_2 Kp}{1+Kp} \tag{2.3}$$

where k_2 is the proportionality constant. This is the simplest treatment of surface reaction. However, in most cases, most surface reactions between two substances follow a bimolecular surface reaction model which is referred to as a Langmuir-Hinshelwood mechanism [10] and represented by the following equation:

$$D.R. = \frac{k_2 KK'PP'}{(1+KP+K'P')^2} \tag{2.4}$$

where P and K are the pressure and proportionality constant of one substance while P' and K' are the pressure and proportionality constant of another substance. If the pressure P' is kept constant, and P is varied, the rate varies in accordance with Figure 1.1 which schematically showed the variation of deposition rate with pressure of one reactant (the other being held constant) for a bimolecular reaction proceeding by a Langmuir-Hinshelwood mechanism (eq.2.4).

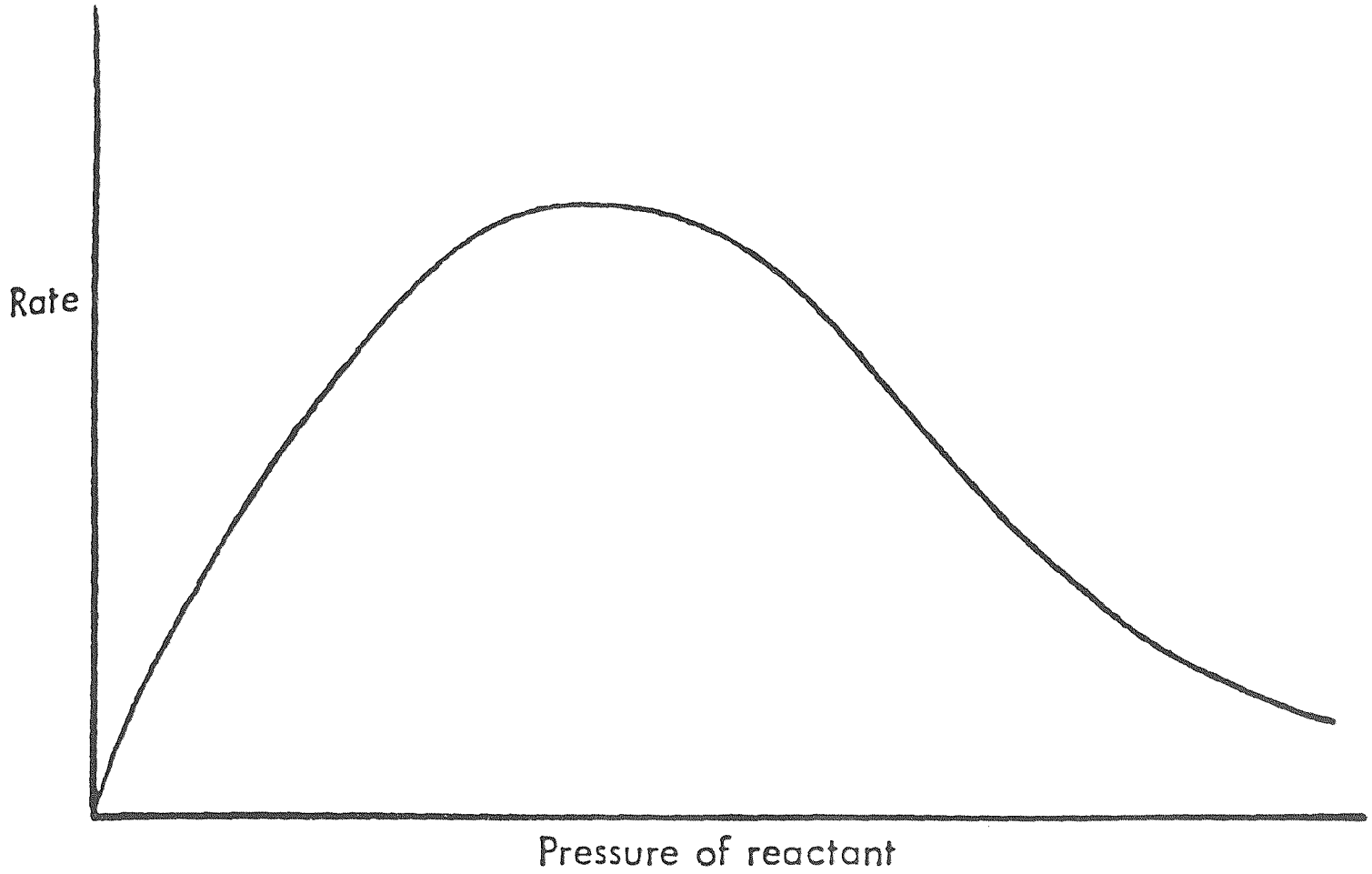

Figure 1.1 Schematic representation of the variation of deposition rate with pressure of one reactant (the other being held constant) for a bimolecular reaction proceeding by a Langmuir Hinshelwood mechanism

The temperature dependence of deposition rate in a heterogeneous mechanism generally follows the empirical Arrhenius behavior of the type :

$$D.R. \propto Ae^{-\frac{Ea}{RT}} \tag{2.5}$$

where A is pre-exponential factor, R is the gas constant, T is the absolute temperature, and E_a is the activation energy [7, 8]. According to this equation, the surface reaction rate increases with increasing temperature. This situation is referred to as a surface reaction rate limited deposition process. However, for a given surface reaction, the temperature may rise high enough so that the reaction rate exceeds the rate at which reactant species arrive at the surface. In such cases, the reaction cannot proceed anymore rapidly than the rate at which reactant species are supplied to the substrate surface by mass transport. This situation is referred to as a mass-transport limited deposition process [7,8]. A typical temperature dependence of deposition rate for a given CVD process is sketched in Figure1.2 [11]. It shows that at high temperatures, the deposition is usually mass-transport limited, while at low temperature it is surface reaction rate-limited. In actual processes, the temperature at which the critical point moves from one growth regime to the other depends on activation energy and gas flow conditions.

1.1.2 CVD Systems

CVD systems generally contain the following components[8]:

a) Gas sources.

b) Gas feed lines.

c) Mass-flow controllers (for metering the gases into the system).

d) A reaction chamber.

e) Means of heating the substrates onto which the film is to be deposited.

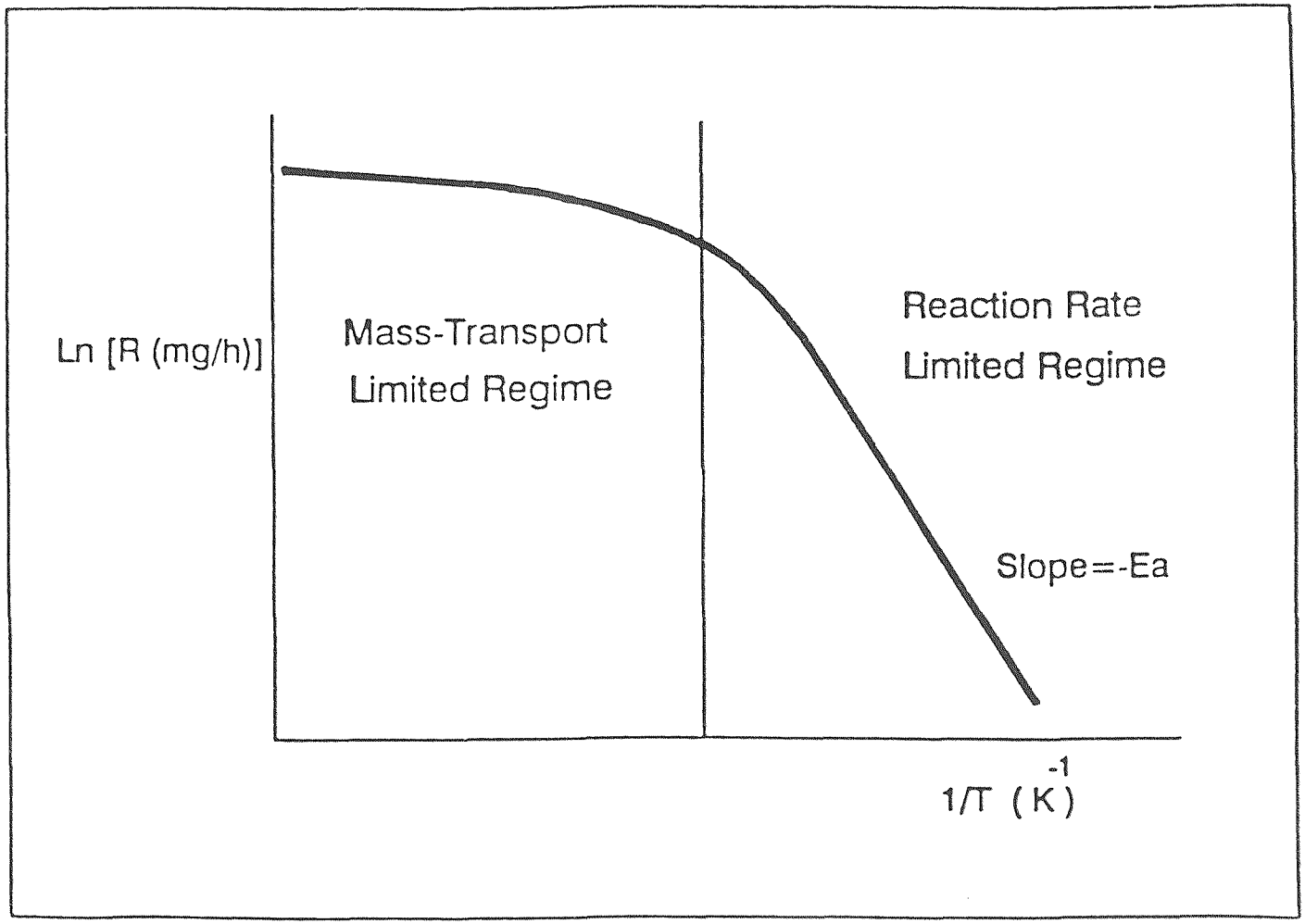

Figure 1.2 Variation of deposition rate as a function of reciprocal temperature for typical CVD process

f) Temperature sensors.

g) Vacuum pumps for achieving reduced pressures and exhausting reactants.

1.1.3 Categories of CVD

1.1.3.1 Introduction

The most important and widely used CVD processes are atmospheric pressure CVD (APCVD), Low pressure CVD (LPCVD), and plasma enhanced CVD (PECVD). In this section, a general description of APCVD and PECVD will be made while detailed discussion of LPCVD will be given as this technique was employed in this thesis work.

1.1.3.2 Atmospheric Pressure CVD (APCVD)

APCVD reactors were the first to be used by the microelectronics industry[12]. Operation at atmospheric pressures kept reactor design simple and allowed high film deposition rates. However, since heterogeneous surface reaction and homogeneous gas phase reaction are of the same order of magnitude in APCVD process, the silicon nitride films synthesized by APCVD typically exhibit poor step-coverage. Currently, APCVD are used only for low temperature oxide (LTO) deposition and epitaxy.

1.1.3.3 Low Pressure CVD (LPCVD)

LPCVD is categorized by its low operating pressure (0.2-2.0 Torr). Most LPCVD process are conducted by resistance heating to attain isothermal conditions so that the substrate and the reactor walls are of similar temperature [7]. The fundamental mechanism underlying the LPCVD process can be explained by the following considerations [13]. The mass transfer of gaseous reactants involves their diffusion across a slowly moving boundary layer adjacent to the substrate

surface. The thinner this boundary layer and the higher the gas diffusion rate, the greater the mass transport that results. Surface reaction rates, on the other hand, depend mainly upon reactant concentration and deposition temperature. The LPCVD boundary layer is thicker by a factor of 3-10 than that of APCVD [7]. Thus, by operating at low pressure (0.20 - 2.0 Torr) and higher temperature (550-850 $^{\circ}$C), LPCVD process enhance mass transfer greatly, making it possible to synthesize films in a highly economical close spaced positioning of the substrate wafers [14]. The surface reaction rate is very sensitive to temperature, but precise control of temperature is relatively easy to achieve.

LPCVD techniques started in 1973 with the work by Tanikawa *et al* [15], who realized from reduced pressure deposition principles that closely packed vertical positioning of the substrate wafers is possible, yielding greatly increased throughput in film deposition for a variety of films without loss of uniformity. In 1975 a patent was issued to Chruma and Hilton [16] for LPCVD of polycrystalline silicon from SiH_4. Since then a lot of efforts were made in the past two decades and which led to the remarkably rapid acceptance of this economical technique for production applications to develop LPCVD techniques.

Basic parameters govern the deposition rate and uniformity of films in LPCVD processes are: 1). temperature profile in the reactor; 2). the pressure level in the reactor; 3). the reactant gas flow rates; and 4). the reactant gas ratios. To obtain a flat thickness profile across each substrate wafer, and from wafer to wafer throughout the reaction chamber, a judicious adjustment of these parameters is required. A precise control of these parameters results in uniform films.

1.1.3.4 Plasma Enhanced CVD (PECVD)

PECVD is categorized by its method of energy input [7]. Rather than relying solely on thermal energy to sustain the chemical reactions, PECVD combines the rf-induced glow discharge process and low pressure chemical vapor deposition to form thin solid films on the substrate surface. An rf-induced glow discharge transfers energy into the reactant gases, allowing the substrate to remain at a lower temperature than APCVD and LPCVD processes. That's the major advantage of PECVD. Desirable properties such as good adhesion, low pinhole density, good step coverage, adequate chemical properties, have led to numerous applications of PECVD films in VLSI fabrication. However, the complexity of reactions associated with PECVD makes the synthesis of stoichiometric compositions difficult. Due to the low deposition temperatures, gases are trapped in the films, which in turn may be the source of thermal instabilities. For examples, in the case of hydrogen, which when released causes deleterious effects on the electronic properties of MOS devices.

1.1.4 The Advantage and Disadvantage of LPCVD

1.1.4.1 The Advantage of LPCVD [7,8]

1). Low pressure operation decreases gas phase reactions, making LPCVD films less subject to particulate contamination and thus have fewer defects and pin holes.

2). A great variety of films including polysilicon, silicon nitride, silicon dioxide, boron nitride, and tungsten can be synthesized by LPCVD.

3). Stoichiometric compositions of the films can be achieved by optimizing LPCVD process parameters.

4). Uniform film thickness and conformal step coverage can be achieved by LPCVD.

5). The cost of LPCVD is economical because of its high throughput and low maintenance cost.

1.1.4.2. The Disadvantage of LPCVD [2]

1). The use of toxic, explosive or corrosive gaseous reactants.

2). The use of comparatively high temperature.

1.2 Properties and Chemical Vapor Deposition of Silicon Nitride Film

1.2.1 Ideal Silicon Nitride Films

1.2.1.1 Stoichiometric Composition

Silicon and nitrogen are the two major constituents of silicon nitride. Oxygen, hydrogen, and carbon are common impurities [17, 18] which affect the stoichiometric composition and quality of the silicon nitride films. Ideal silicon nitride films should have a stoichiometric composition where the Si/N ratio is 0.75 and should be stable under high temperature and harsh chemical processing conditions.

1.2.1.2 Refractive Index

The refractive index of silicon nitride films is 2.0 and a good indicator of stoichiometry. The reported refractive index of LPCVD silicon nitride films is in the range of 2.0 - 2.1, while the refractive index of PECVD silicon nitride films is in the range of 1.8 to 2.5 [18].

1.2.1.3 Density

The density of silicon nitride films ranges from 2.4 to 3.1g/cm^3[18]. It serves as an indicator of the concentrations of impurities and pinholes in the deposits. The density of LPCVD silicon nitride films ranges from 2.8 to 3.1 g/cm^3, while the

density of PECVD silicon nitride films ranges from 2.4 to 2.8 g/cm^3.[18].

1.2.1.4 Thickness Uniformity and Conformal Step Coverage

Film thickness uniformity and conformal step coverage are two basic requirements for manufacturing high quality electronic devices with reliable electrical properties and long lifetimes.

1.2.1.5 Electrical Properties

The electrical properties of silicon nitride films are derived from studies of Metal (Al, Au, Ag) - Nitride (Si_3N_4) - Semiconductor (Si) capacitor (MNS) [2]. The dielectric constant ε is estimated from the relation $\varepsilon = Cd / \varepsilon_o A$ where C is the capacitance, d is the thickness of the Si_3N_4 thin film layer, A is the area of capacitor, and ε_o is the free space dielectric permittivity ($8.8*10^{-14}$ Fcm^{-1}). For silicon nitride films, the value for the dielectric constant varies from 6 to 9. Silicon nitride has a high dielectric breakdown voltage. The value is approximately 10^7 Vcm^{-1} [2]. This is essential for good insulation. When a constant voltage is applied across a dielectric layer, a high dielectric permittivity reduces the electric field strength in the film. Thus, increasing the dielectric permittivity results in an increase in the breakdown voltage which benefits device performance.

1.2.1.6 Ideal Stress

High stress causes deterioration in device reliability. Films with a high tensile or compressive stress tend to crack or peel. The ideal stress for films used in passivation devices is compressive between $2*10^9$ and $5*10^9$ dyne/cm^2 and the ideal films used as membranes for x-ray masks are tensile between $1*10^9$ and $5*10^9$ dyne/cm^2[19].

1.2.2 Application of Silicon Nitride Films

Silicon nitride films are amorphous insulating materials that are used in three primary VLSI applications:

1) As chemically and electrically stable passivation layers on integrated circuits in order to withstand corrosive reactions and prevent ion diffusion [20, 21, 22].
2) As masks in semiconductors to protect against donor and acceptor impurity diffusion [23] as well as masks to protect against oxidation since the silicon nitride films oxidize very slowly [18,24].
3) As a gate dielectric over thermally grown dioxide in dual dielectric devices [17, 22].

Silicon nitride is highly suitable as a passivation layer because of its following properties:

a) It behaves as a nearly impervious barrier to diffusion (in particular, moisture and sodium find it very difficult to diffuse through the nitride film).
b) It can be prepared by PECVD to have a low compressive stress, which allows it to be subjected to severe environmental stress with less likelihood of delamination or cracking.
c) Its coverage of underlying metal is conformal.
d) It is deposited with acceptably low pinhole densities.

Silicon nitride is useful as masking for selective oxidation, because it is difficult for oxygen to penetrate silicon nitride. The silicon nitride itself oxidizes very slowly, but it is not penetrated by oxygen.

Furthermore, silicon nitride can also be used as dielectric and anti-reflection coatings for solar cells and photo-detectors [25,26]; as etching masks in multi-level resist structure [27]; as supporting membranes for x-ray lithography masks [28].

1.2.3 Chemical Vapor Deposition of Silicon Nitride Films

1.2.3.1. The History of Chemical Vapor Deposition of Silicon Nitride Films

It appears that the first published successful attempt to prepare silicon nitride films is the work of Sterling and Swern [16] in 1965. They synthesized silicon nitride films from the mixture of silane and anhydrous ammonia using rf-discharge assisted CVD. Before the advent of LPCVD, silicon nitride films were synthesized by CVD at atmospheric pressures around 900 °C from a variety of reactants. V. Y. Doo, D. R. Nichols, and G. A. Silvey synthesized silicon nitride films by APCVD from SiH_4-NH_3-H_2 precursor systems in 1966 [29]. K. E. Bean, P. S. Glein, and R. L. Yeakley reported their CVD work of synthesizing silicon nitride films from SiH_4-NH_3-H_2 precursor system in 1967 [30]. The synthesizing of silicon nitride films on silicon substrates from $SiCl_4$-NH_3 precursor systems was reported by M. J. Grieco and et al in 1968 [31], and by V. D. Wohlheiter in 1972 [32]. With the advent of LPCVD techniques in 1973, Tanikawa *et al* first reported the low pressure deposition of silicon nitride films using SiH_4-NH_3 precursor system in 1973 [15], but with no detail on the effects of deposition parameters on the film characterizations was shown in this paper. Up to 1977, R. S. Rosler reported the synthesizing of amorphous silicon nitride films by LPCVD from SiH_2Cl_2-NH_3 precursor systems [14]. Following this discovery, a large number of LPCVD silicon nitride films synthesized from SiH_2Cl_2-NH_3 precursor system had been reported including P. Pan and W. Berry in 1985 [20], K. F. Roenigk and K. F. Jensen in 1987 [33], S. L. Zhang, J. T. Wang, W. Kaplan , and M. Ostling in 1992 [34].

1.2.3.2.Comparison of the Properties and Usage of Silicon Nitride Films Deposited by LPCVD and PECVD

Currently, LPCVD and PECVD are two most importantly and widely used CVD

processes to obtain silicon nitride films. Table 1.1 [18] compares the properties of LPCVD and PECVD silicon nitride films. We can conclude from this table, when silicon nitride used as a mask for selective oxidation or as a gate dielectric material, silicon nitride film is generally deposited by high-temperature LPCVD techniques, for reasons of film uniformity and lower processing cost [35]. When used as a passivation layer, the deposition process must be compatible with such low-melting-point metals as aluminum. Thus silicon nitride must be deposited by PECVD as it can deposit silicon nitride films at 200 - 400 °C [36, 37]. Nevertheless, PECVD silicon nitride is generally nonstoichiometric and contains high quantaties of hydrogen (10-30%) and is chemically represented as $Si_xN_yH_z$. We can see from the refractive index values of this table that LPCVD tends to produce stoichiometric films while the broader values for the refractive index of PECVD silicon nitride reflects formation of non-stoichiometric films.

1.3 LPCVD of Silicon Nitride Films

The advantages of LPCVD Synthesis were discussed in section 1.1 which indicates that LPCVD has the advantage over PECVD of producing stoichiometric silicon nitride films at relatively lower costs. However, the deposition temperatures associated with LPCVD are relatively higher than those of PECVD. LPCVD silicon nitride films have higher density (2.8 - 3.1 g/cm^3), and higher dielectric constants than PECVD silicon nitride films. Furthermore, they exhibit excellent step coverage and relatively low particulate contaminations. As we review the history of precursors used in LPCVD silicon nitride, silane was the original choice precursor followed later by the halogen containing sources $SiCl_4$ and SiH_2Cl_2 [38]. Silane is highly toxic, flammable, and pyrophoric; $SiCl_4$ is corrosive; SiH_2Cl_2 is flammable and corrosive [39]. Furthermore, their use requires expensive gas cabinets and

cross purging gas supply systems to insure safety and prevent corrosion of vacuum pumps. The search for a safer and less corrosive precursor is, thus, of great interest to the semiconductor industry.

Table 1.1 Properties of LPCVD and PECVD deposited silicon nitride films [9]

Property	LPCVD	PECVD
Deposition temperature	550 - 850 °C	200 - 400 °C
Composition	Si_3N_4	$Si_xN_yH_z$
Si/N ratio	0.75	0.8 - 1.0
Refractive index	2.0 - 2.1	1.8 - 2.5
Dielectric constant	6-7	6-9
Dielectric strength	$1*10^7$ V/cm	$6*10^6$ V/cm
Stress (dyne/cm^2)	$1.2 - 1.8*10^{10}$ (tensile)	$1 - 8*10^9$ (compressive)
H_2O permeability	zero	Low-none
Thermal stability	Excellent	Variable > 400 °C
Density (g/cm^3)	2.8 - 3.1	2.5 - 2.8
Step coverage	conformal	good
Si-N max	870 cm^{-1}	830 cm^{-1}
Si-H minor	None	2180cm^{-1}

1.4 Objectives of This Thesis Work

In this thesis, ditertiarybutylsilane (DTBS) with a chemical formula $SiH_2(C_4H_9)_2$ is used in the presence of ammonia (NH_3) to produce silcon nitride films by

LPCVD. DTBS is a colorless, air stable, non-toxic, and non-corrosive liquid. It is, thus, a safe precursor with promising properties as a suitable substitute for silane and other halogen sources. Table 1.2 concludes the properties of DTBS.

Table 1.2 Properties of DTBS [39]

Chemical name	ditertiary butyl-silane (DTBS)
Chemical formula	$SiH_2 (C_4H_9)_2$
Chemical family	Organic silane
Chemical description	Colorless liquid
Solubility in water	Slight
Volatile	100%
Boiling point	128 °C
Flash point	15 °C
PH Factor	5 - 6
Vapor pressure	20.5 Torr (@ 20 °C)

As to technical feasibility, DTBS had already been used in hot wall horizontal LPCVD to deposit chemically stable silicon nitride films by its manufacturer — Olin Hunt company [39]. Silicon nitride films with an average thickness of 2844 Å were successfully synthesized by LPCVD from DTBS (50 sccm) and NH_3 (18 sccm) at a temperature of 650 °C and total pressure of 1.7 Torr. The measured average refractive index value of 1.956 reflected the stoichiometric composition of the deposited silicon nitride film. These promising preliminary results provided the incentive for a further pursuit of this work.

CHAPTER 2

EXPERIMENTAL PROCEDURES

2.1 Set-up of LPCVD System

The LPCVD reactor shown in Figure 2.1 was used to deposit the silicon nitride films of this study. The reaction chamber consists of a fused silica tube, having an inner diameter of 12.5 cm and a length of 120 cm. It was mounted horizontally within a three zone Lindberg furnace capable of operating at a maximum temperature of 1200 $^{\circ}$C. The fused silica tube which was sealed on both ends by water cooled O-ring caps was separated from coils by a ceramic enclosure. A type K (nickel-aluminum vs nickel-chromium) thermocouple was used to measure temperature. An MKS mass flow controller Model 8240 and an MKS 200 sccm vapor phase flow controller Model 1150B-162M were used to measure and control the flow rate of ammonia and DTBS respectively. The pressure in the reactor was monitored by an MKS Baratron pressure gauge. An Edwards two-stage vacuum station comprised of a mechanical pump Model E2M40 and a booster pump Model EH 250 was used to establish the required vacuum. An oil filter system was used to filter unnecessary particles from the pump oil and thereby increase the lifetime of the pumping system.

2.2 Pre-deposition Procedure

2.2.1 Leak Check

A leak check was conducted at the beginning of every experimental run to avoid oxygen and insure formation of films with desirable and reproducible quality. During this leak check procedure, all pneumatic valves, mass flow controllers, and gas regulators were fully open. After sealing the outlet of the reaction

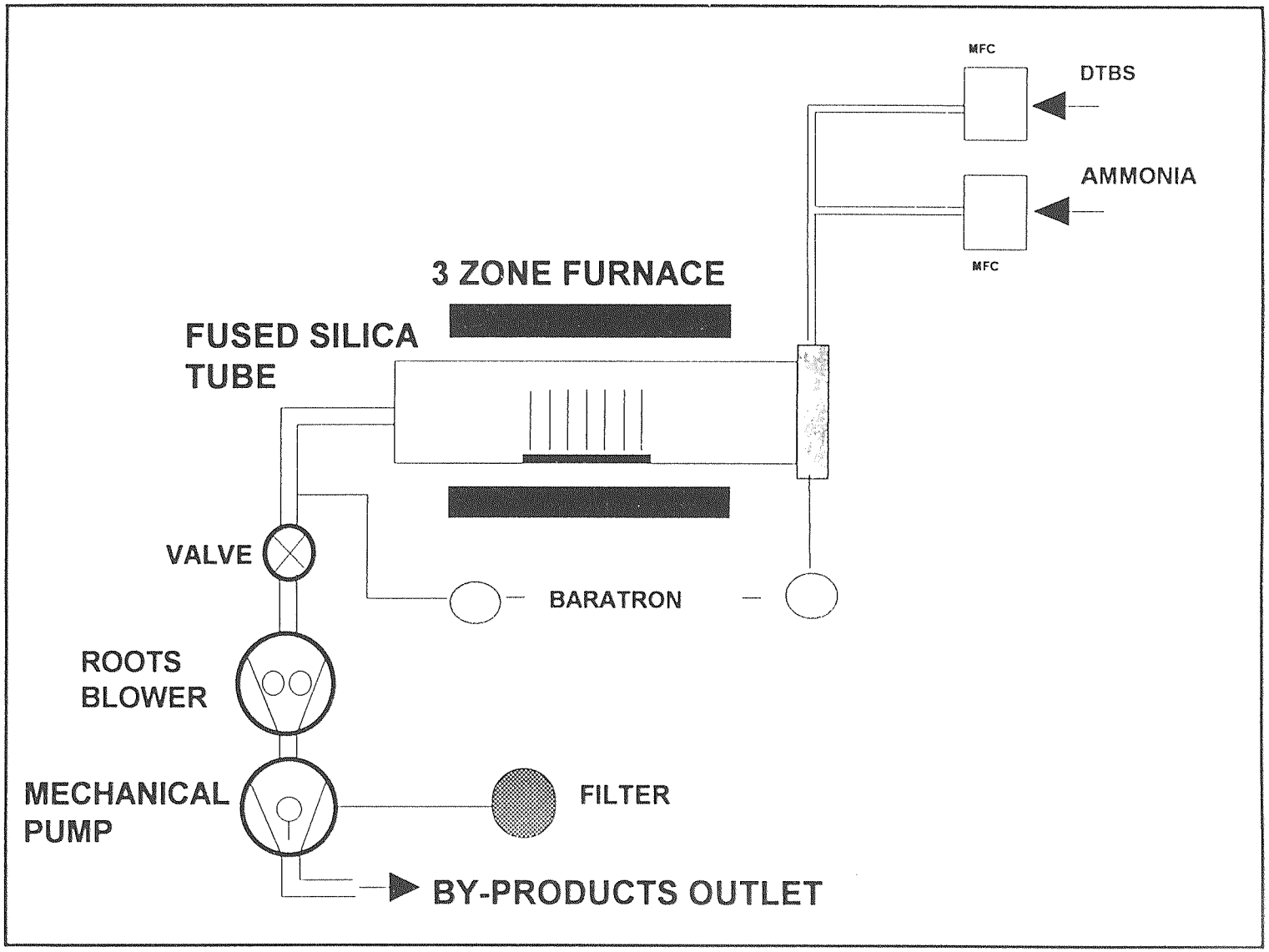

Figure 2.1 Schematic of LPCVD reactor used to synthesize silicon nitride films

chamber, the pressure rise in the reactor was measured and the leak rate calculated. Typical leak rates were on the order of 5 mtorr/min which was deemed acceptable.

2.2.2 Temperature Calibration of the Reaction Chamber

In order to calibrate temperature, a calibrated type K thermocouple was introduced into the reaction chamber from a inlet in the front end-cap. Readings were taken every 5 cm along a 35 cm length of the central zone as shown in Figure 2.2. A 20 minute wait took place between readings to insure temperature equilibrium.

2.2.3 Flow Rate Calibration

Flow rate for the reactants was established with aid of the ideal Gas Law:

$$PV = nRT \tag{2.1}$$

Assuming the room temperature is T_r and taking it as the reaction chamber temperature. Since chamber volume V were fixed, then

$$\frac{P}{n} = \frac{R * T_r}{V} = const \tag{2.2}$$

$$\frac{\partial n}{\partial t} = \frac{V}{R * T_r} * \frac{\partial P}{\partial t} \tag{2.3}$$

where t is time. At standard condition of temperature (273 °K) and pressure (760 Torr),

$$V_s = \frac{nRT}{P} = nR * \frac{273}{760} \tag{2.4}$$

$$\frac{\partial V_s}{\partial t} = R * \frac{273}{760} * \frac{\partial n}{\partial t} \tag{2.5}$$

Substitute equation (2.3) into (2.5), one obtains:

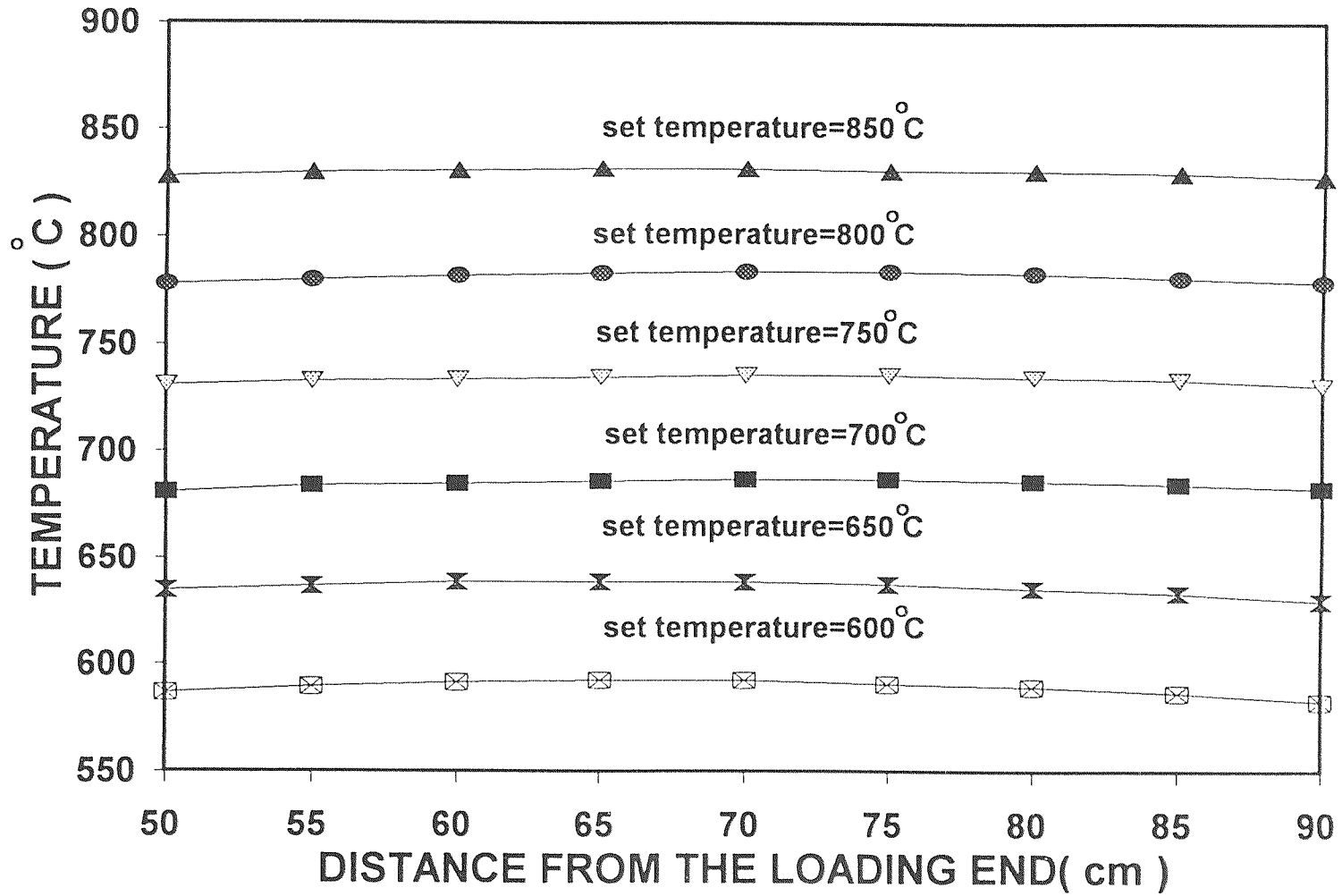

Figure 2.2 Temperature profile of LPCVD reaction chamber

Flow rate at room temperature of T_r

$$F.R. = \frac{\partial V_s}{\partial t} = \frac{V}{760} * \frac{273}{T_r} * \frac{\partial P}{\partial t} \tag{2.6}$$

Then,

$$\frac{760}{V} = \frac{\Delta P / \Delta t}{F.R.} * \frac{273}{T_r} \tag{2.7}$$

Where V is the volume of the reaction chamber, T_r is the measured room temperature and $\Delta P/\Delta t$ is the pressure variation rate. Equation 2.7 was used to calibrate the flow rate of each reactant gas. The calibration procedure was carried out at measured room temperature. The reaction chamber was kept at room temperature and pumped down for about 30 minutes, the flow rate was then set, the gas line opened to introduce the gas into the reaction chamber, and the outlet valve of the chamber valve closed. In an ideal gas situation, the reactant gas flow rate can be obtained by measuring the pressure variation rate $\Delta P/\Delta t$ since chamber volume are known.

2.3 LPCVD Experimental Procedure

2.3.1 Wafer Loading

Deposition was carried out on 10 cm diameter single crystal <100> silicon wafers positioned in an upright position on a fused silica boat. The front boat was placed in the reaction chamber at a distance of 55 cm from the loading end. There were 12 single wafer slots and 11 double wafer slots on the boat. The spacing between the adjacent single and double wafer slots is 1.25 cm while the spacing between the adjacent single wafer slots (or double wafer slots) is 2.5 cm. Four virgin wafers consisting of three Si and one quartz were placed at the same location in each run to maintain reproducible experimental conditions. As shown in figure 2.3, four virgin wafers were separated through the reactor by four "dummy" wafers. The first "dummy" wafer was placed on third single wafer

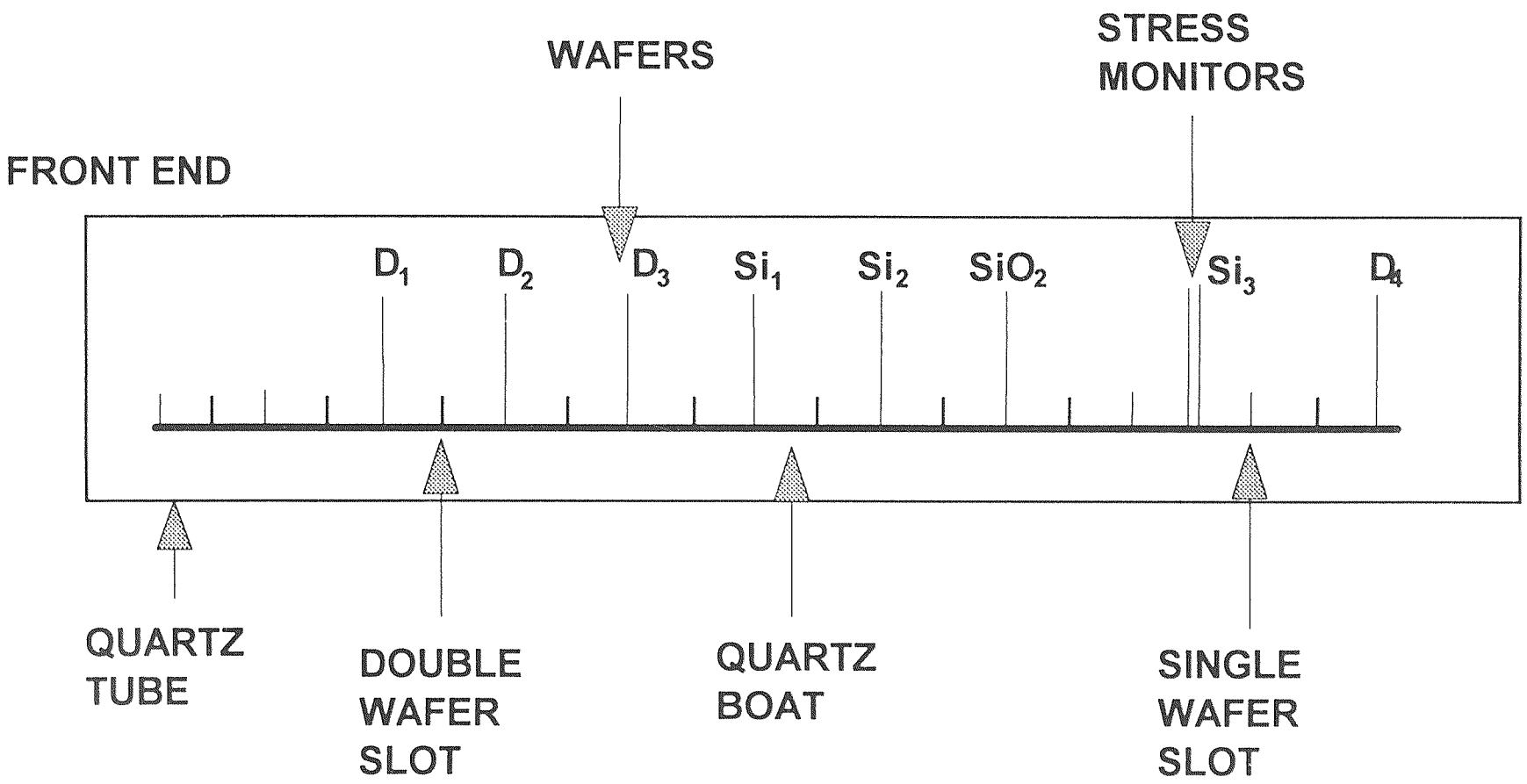

Figure 2.3 Wafer loading scheme used within reaction chamber
D_1: 1st dummy wafer; D_2: 2nd dummy wafer D_3: 3rd dummy wafer D_4: 4th dummy wafer
Si_1: 1st silicon wafer; Si_2: 2nd silicon wafer; Si_3: 3rd silicon wafer

slot which is 9 cm from the end of the boat. The first virgin wafer was located on the sixth single wafer slot right after first three "dummy" wafers. The third virgin wafer was placed back to back on double wafer slot with a <111> Si wafer and was dedicated for the stress measurement. The fourth virgin wafer was quartz and was used for subsequent optical transmission measurements.

All wafers were weighed accurately to 0.1 mg before and after deposition to obtain the weight gain needed to calculate deposition rate and evaluate the degree of depletion in each run. The radius of curvature was measured on the stress monitor before and after each deposition to determine stress values.

2.3.2 Heating and Deposition Condition Setting

After loading the wafers, the reaction chamber was evacuated for about one hour. Cooling water and running fans were used to cool the O-rings and plastic parts of the chamber. The reaction chamber was then heated to the desirable deposition temperature (about 2 hours) and stabilized for thirty minutes. Meanwhile, the gas feed lines as well as valves were checked and flow rates of DTBS and ammonia set. The vapor mass flow controller was warmed up and made ready for DTBS flow.

2.3.3 Film Deposition

Ammonia was first introduced into the reaction chamber for about 2 minutes prior to introduction of the DTBS. As soon as the DTBS was introduced, the desired total pressure of the reaction chamber was adjusted to the desired value by manually operating the exhaust valve and maintaining it constant throughout the entire deposition process. At the end of deposition, the samples were cooled overnight before removing them from the chamber.

2.4 FILM CHARACTERIZATION TECHNIQUES

2.4.1 Physical Properties

Film thickness was measured by Nanospec Interferometry which is based on the production of monochromatic light interface fringes in a space limited by the sample surface and a semi-transparent mirror. Density of the silicon nitride films was determined from the slope of a plot of film thicknesses versus weight gain.

2.4.2 Compositional Properties

The elemental composition and chemical states were studied by X-ray Photoelectron Spectroscopy (XPS) and Rutherford Backscattering Spectroscopy (RBS) measurements.

In the XPS measurement, low energy X-rays such as $K\alpha$ line of aluminum at the energy level of 1.487 Kev can be employed to bombard the sample and cause photoelectron emission. The X-ray photo energy removes an inner shell electron from an atom when it is absorbed. The electron is emitted with a kinetic energy characteristic of the difference between the X-ray and the binding energy of the electron. The energy of the emitted electron defines the type of the atom and the number of electrons at this energy is related to the density of the atoms present. XPS can be used to examine several top monolayers of thin film and provide information about the chemical bonding of the elements. The limitation of the XPS is that it cannot detect hydrogen and helium sinc the XPS measurement process involving the excitation and emission of at least 3 electrons.

XPS can be used to obtain information about chemical bonding and composition. In the analyses of as-deposited silicon nitride films, the atomic concentration data were collected using XPS individual peak spectra after etching 200Å from the surface.

The Rutherford Backscattering Spectroscopy (RBS) measurements were taken using a High Voltage Engineering AK accelerator with He^+ ions at an energy of 1.8 Mev to corroborate the XPS data. The RBS technique is essentially nondestructive and no standard sample is needed. Elastic collisions occur between the high energy incident ions and the outer surface and subsurface atoms of the sample. Upon colliding, some of the incident ions are backscattered and experience an energy loss that is characteristic of the atom with which they collide. Thus, from the energy of the backscattered ions, elemental analysis can be determined.

2.4.3 Structural Properties

The structural configuration of the silicon nitride films was established by X-ray diffraction measurements conducted with a Cu target on a Philips XRG 3100 system operating at 45 KV and 40 mA. Optical microscopy was used to inspect for the possible presence of cracks, gas phase nucleation clusters, and other defects in the deposits.

2.4.4 Optical Properties

The IR spectra were taken using a Perkin Elmer 1600 series FTIR spectrophotometer while the optical transmission was calculated from the Ultraviolet/Visible absorption spectroscopy data measured with a Varian DMS 300 spectrophotometer. The refractive index values were measured with a Rudolph Research/AutoEL ellipsometer which is made up of a monochromatic light source, a collimator, a polarizer which polarizes the light, a compensator which transforms the linearly polarized light, a support on which the sample is placed, an analyzer, and a detector.

2.4.5 Mechanical Properties

Film stress was determined with a home built system that measured changes in the radius of curvature of a wafer resulting from deposition on a single side. figure 2.4 shows an optical imaging system for setup. The distance between two points generated by light from two fixed and parallel He-Ne lasers was determined after reflection from the surface of a wafer before and after deposition. An angled mirror was used to project the reflection of the two points onto a wall where their separation could be more actually measured.

The hardness and Young's modulus of as-deposited silicon nitride films were obtained using a Nano Instruments Indenter. As shown in figure 2.5, The system consists of a triangular pyramid-shaped diamond tip mounted on a loading column. A coil and magnet assembly were located on the top of the loading column to provide a controlled loading force. The force imposed on the column which is suspended by flexible springs is controlled by varying the current in the coil. The position of the indenter is determined by a capacitance displacement gauge which is very sensitive to detect the trivial displacement change.

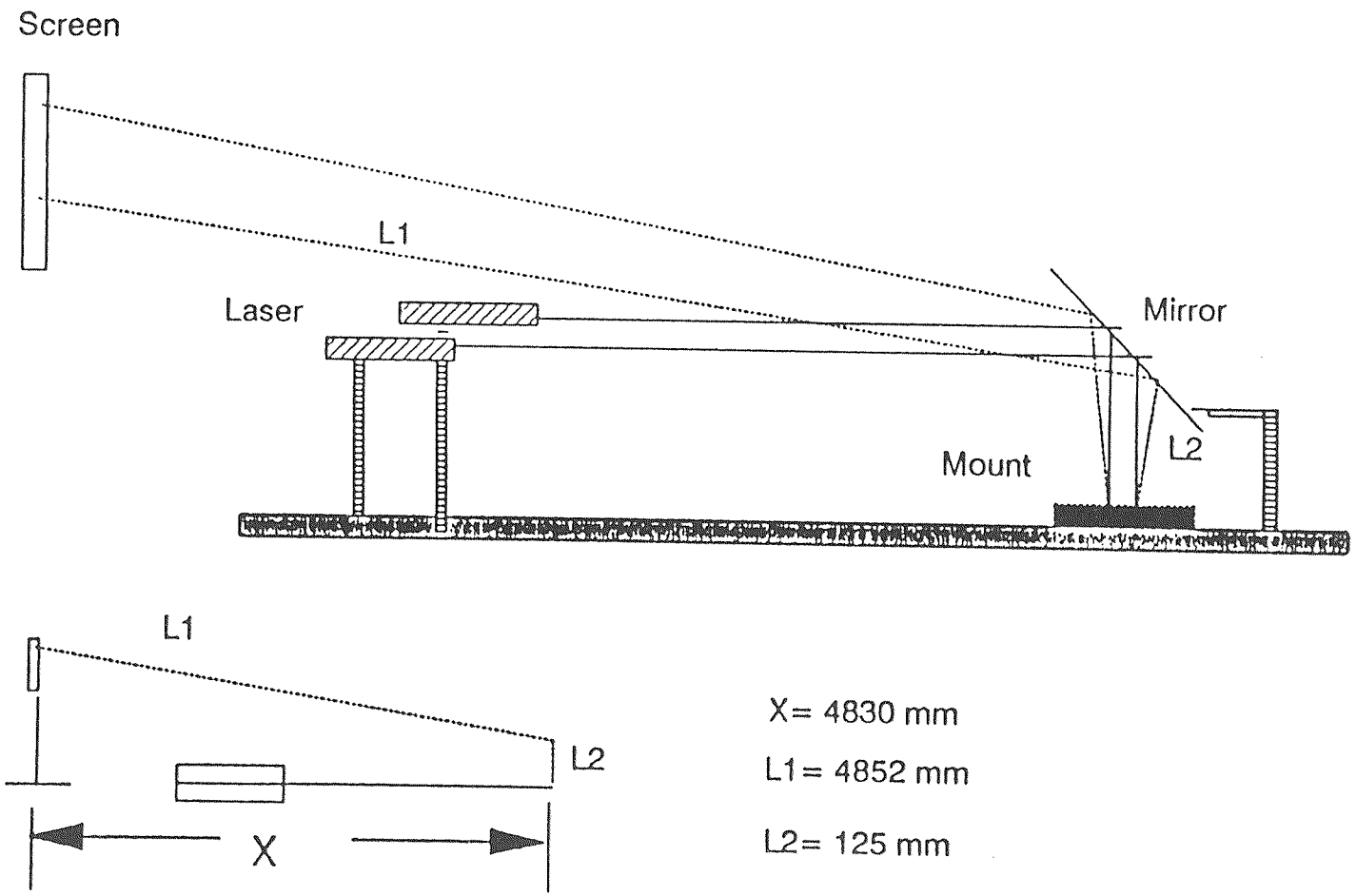

Figure 2.4 Optical system for stress measurement setup

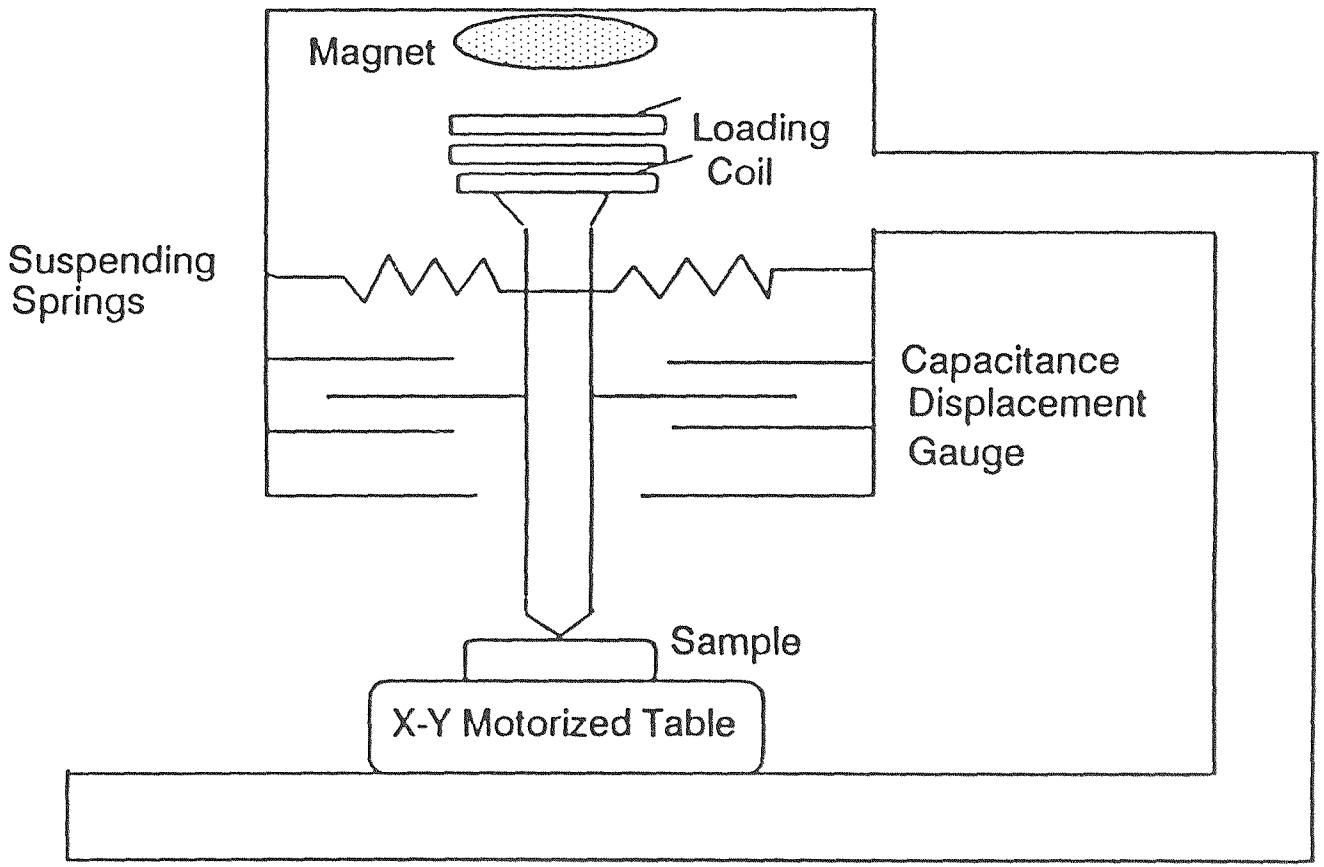

Figure 2.5 Schematic of the indenting mechanism of Nano Instrument Indenter

CHAPTER 3

RESULTS AND DISCUSSIONS

3.1 The Effects of Deposition Variables on Film Deposition Rate and Film Composition

The deposition rates were investigated as a function of processing parameters in which DTBS flow rates were varied over the range of 10 to 50 sccm, NH_3 flow rates over the range of 50 to 250 sccm, pressures over the range of 0.2 to 1.1 Torr, and temperatures over the range of 600 to 900 °C. In this study, the deposition rates, expressed in Å/min, are presented for the three Si wafers used in each run to illustrate the degree of depletion across the reaction chamber.

RBS and XPS analyses were carried out at Bell laboratory and Olin Hunt Inc. respectively to obtain the compositional values of silicon nitride films.

Figure 3.1 shows a typical RBS spectrum for a silicon nitride film deposited at the temperature of 650 °C, pressure of 0.5 Torr, DTBS flow rate of 10 sccm, and NH_3 flow rate of 100 sccm. The X-axis shows the backscattered energy and the Y-axis shows the normalized yield. The result of the percent composition of each element was obtained by comparing the amplitude of the peak corresponding to the energy level for its standard pure element.

Figure 3.2 shows an XPS spectrum of a silicon nitride film deposited at the temperature of 650 °C, pressure of 0.5 Torr, DTBS flow rate of 10 sccm, and NH_3 flow rate of 150 sccm. The X-axis shows the binding energy of the emitted electrons. The Y-axis shows intensity level. Silicon and nitrogen percentage was estimated by the level of peaks corresponding to its binding energy level. Previous work has shown that when Si_3N_4 is Ar ion etched it has about a 1:1 Si:N atomic concentration ratio. The spectra displayed the Si_3N_4 character

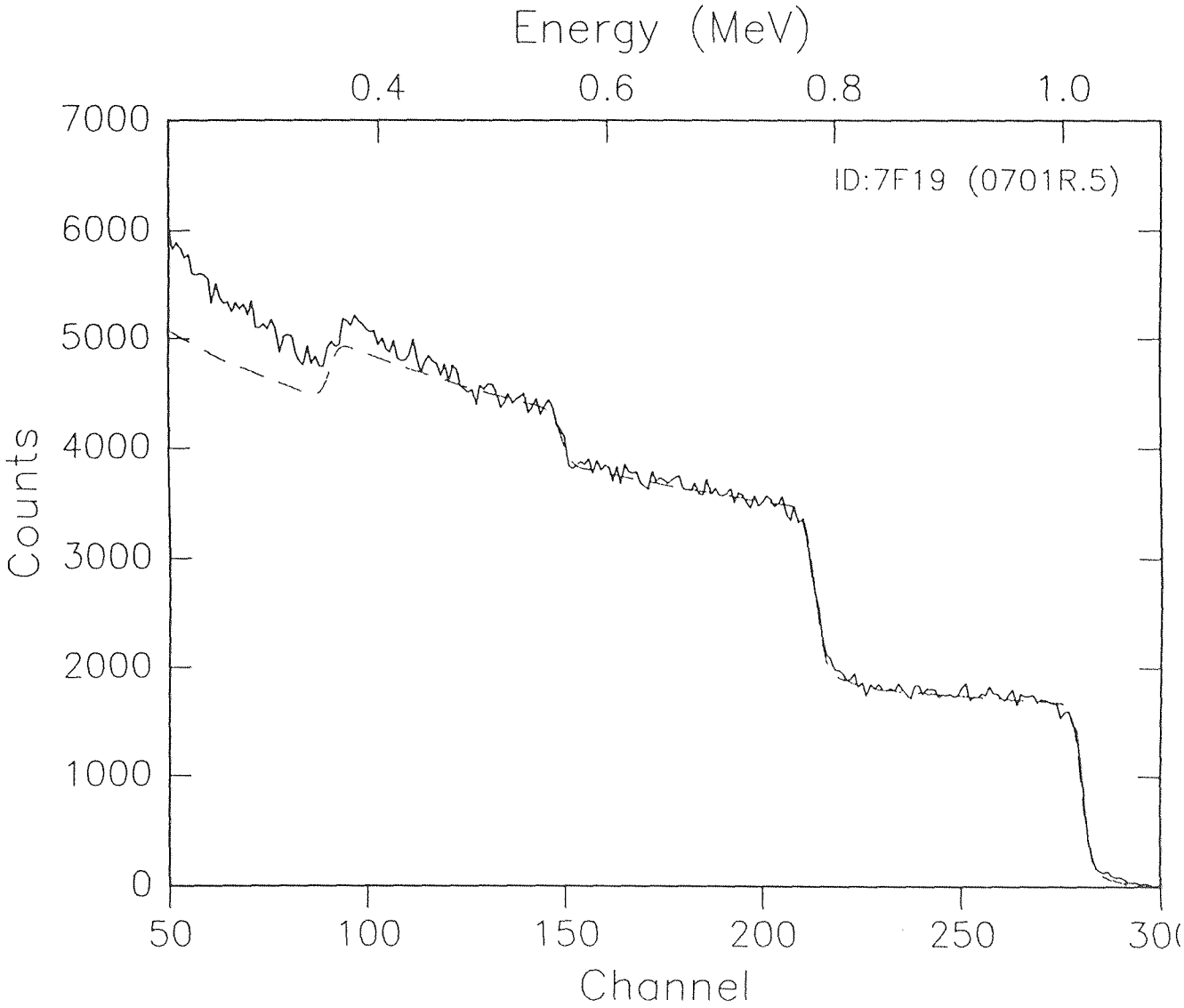

Figure 3.1 A typical RBS spectrum for a silicon nitride film deposited at a temperature of 650 °C, pressure of 0.5 Torr, DTBS flow rate of 10 sccm, and NH_3 flow rate of 100 sccm.

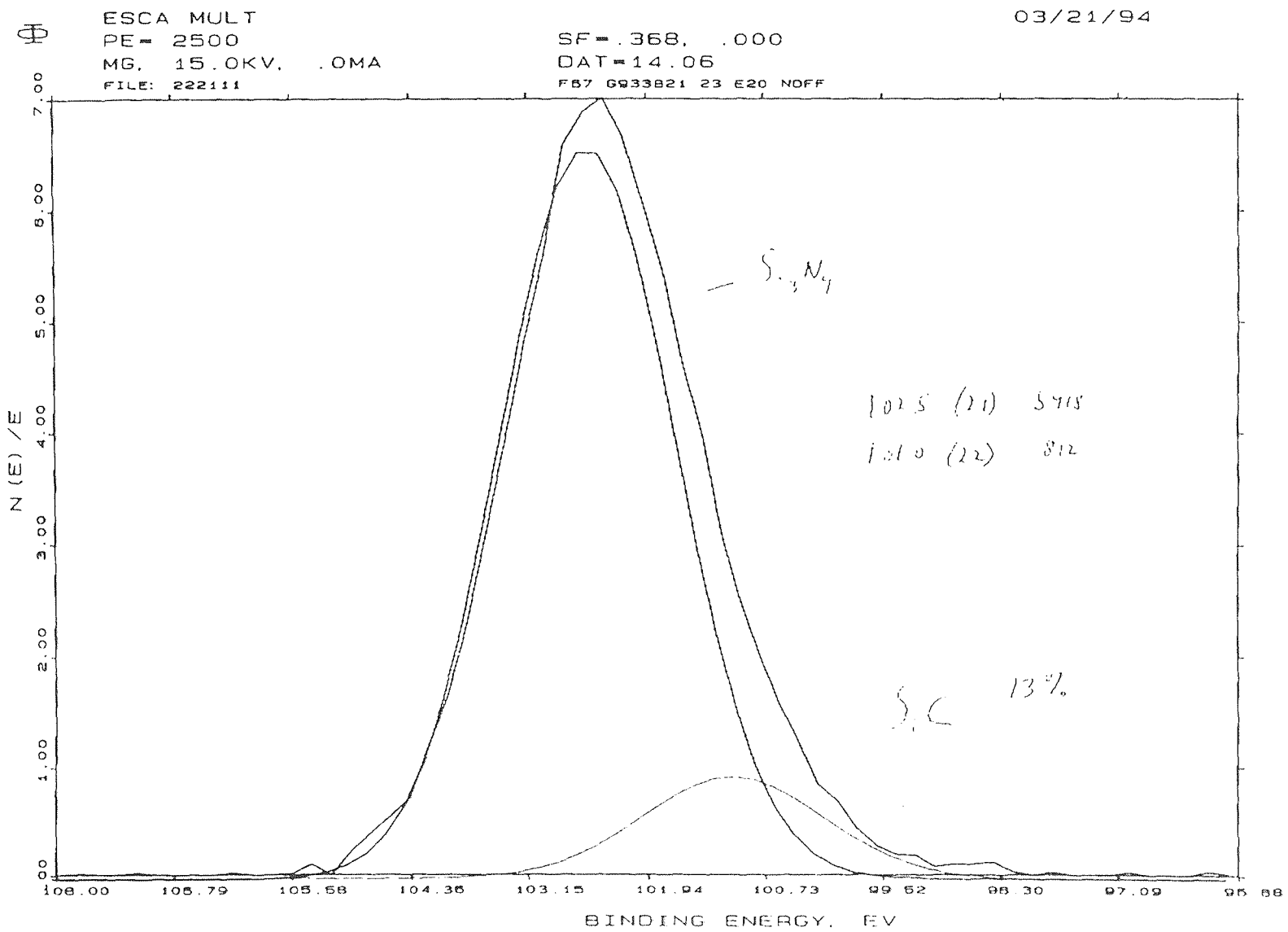

Figure 3.2 XPS spectrum for a silicon nitride film deposited at a temperature of 650°C, pressure of 0.5 Torr, DTBS flow rate of 10 sccm and NH_3 flow rate of 150 sccm.

consistently. Additionally, four film samples were depth profiled and good uniformity of composition were found.

3.1.1 Temperature Dependent Study

The temperature dependent behavior of deposition rate is shown in figure 3.3 while the temperature dependent behavior of atomic concentration of silicon, nitrogen and carbon is shown in figure 3.4. For a constant DTBS flow rate of 10 sccm, NH_3 flow rate of 100 sccm and pressure of 0.5 Torr, the deposition rate is seen to follow an Arrhenius type behavior in the temperature range of 600 to 700 $^{\circ}C$ that yields an activation energy of 50.2±0.2 kcal/mol. This calculated activation energy is comparable to the value of 37.5 kcal/mol reported for silicon nitride films synthesized from dichlorosilane (SiH_2Cl_2) and ammonia (NH_3) [33]. At temperatures above 700 $^{\circ}C$, the deposition rate was observed to decrease reflecting a combination of factors including the transition into the mass transfer limited regime and gas phase nucleation effects. As seen in Fig. 3.3, depletion across the reaction chamber is negligible over the entire temperature regime investigated, thus, qualifying this process as a high throughput one.

As seen in figure 3.4, stoichiometric silicon nitride film can be obtained over the entire temperature range of 600-900 $^{\circ}C$. Furthermore, the compositions of silicon nitride films had almost no fluctuation even above 700 $^{\circ}C$, however, the deposition mechanism tend to change to the mass transfer limited regime and more byproducts were created above 700 $^{\circ}C$. This phenomenon indicates that gaseous byproducts had not been adsorbed by the heated substrates on which stoichiometric silicon nitride films formed. Instead, these gaseous byproducts were exhausted by the pumping system.

It is interesting to note that the lowest temperature for depositing silicon nitride film occurs in the case of DTBS at 600 $^{\circ}C$ which is at least a 100 $^{\circ}C$ lower

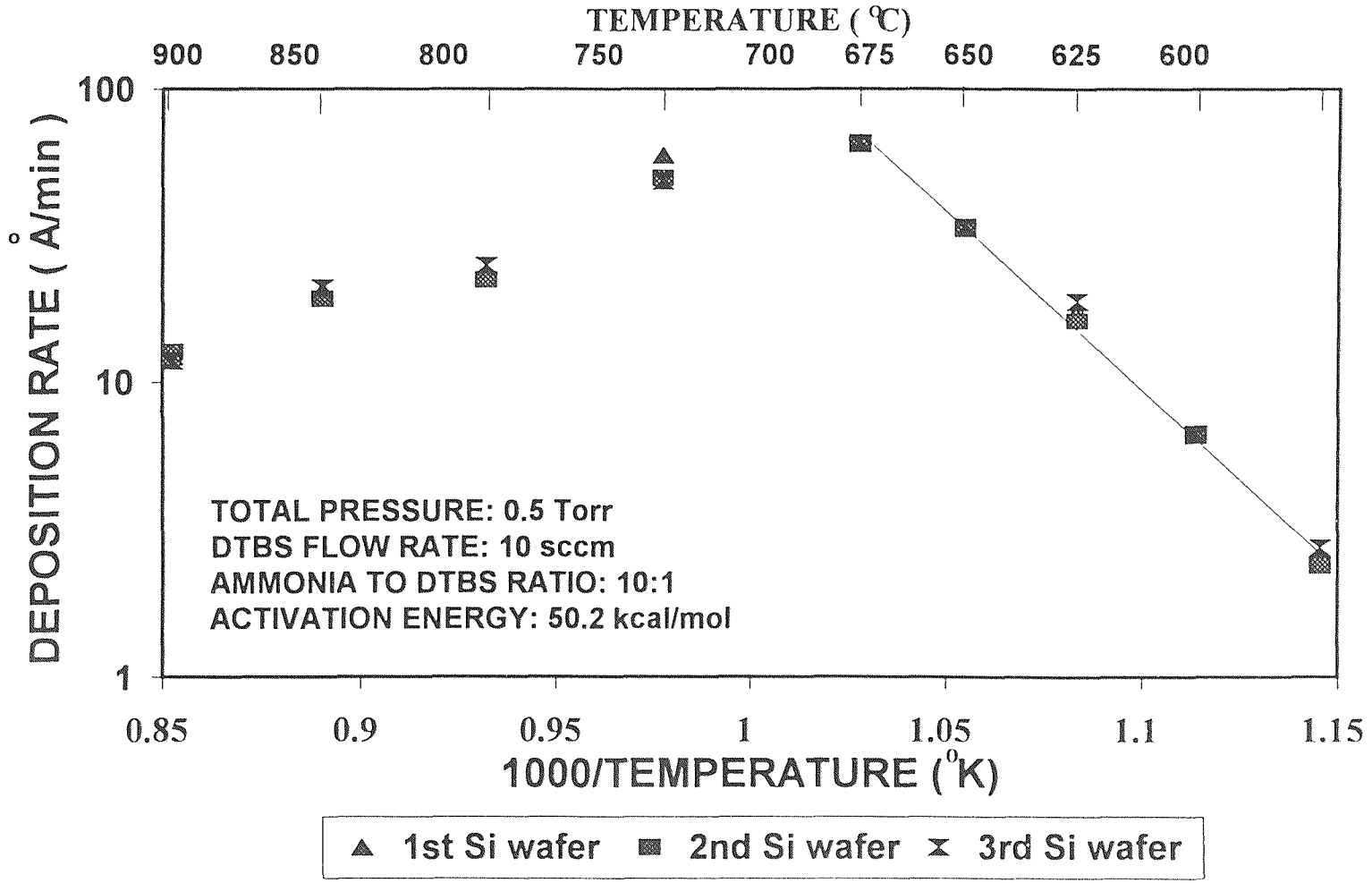

Figure 3.3 Variation of deposition rate of silicon nitride films as a function of reciprocal temperature

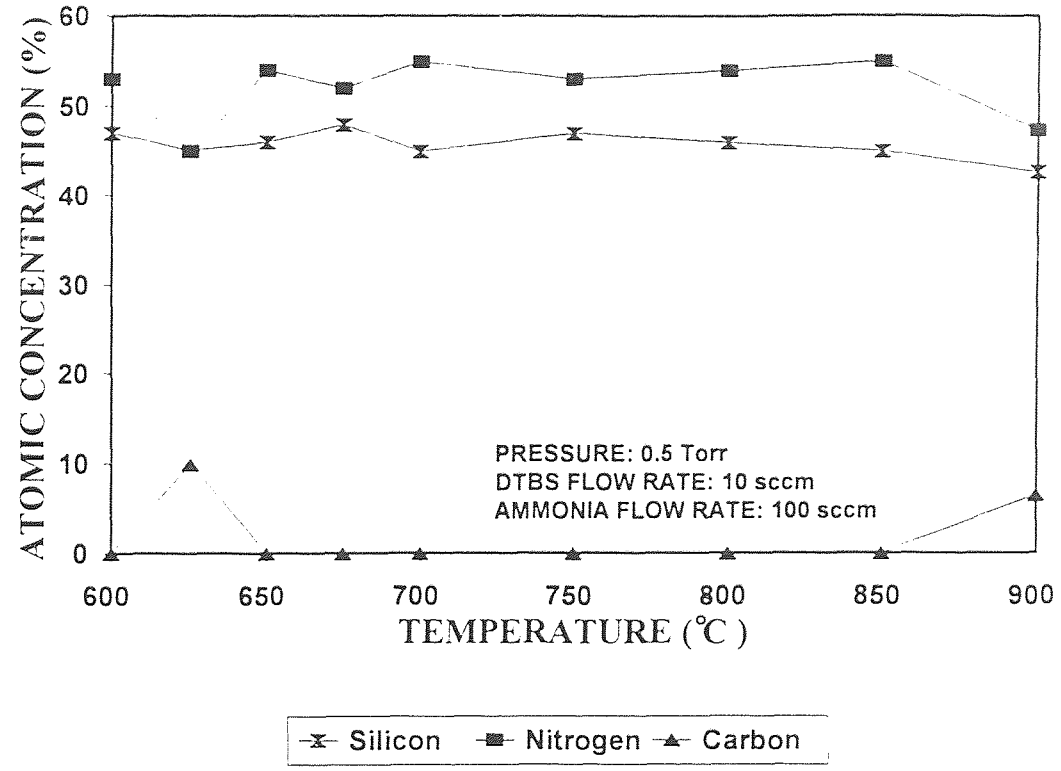

(a)

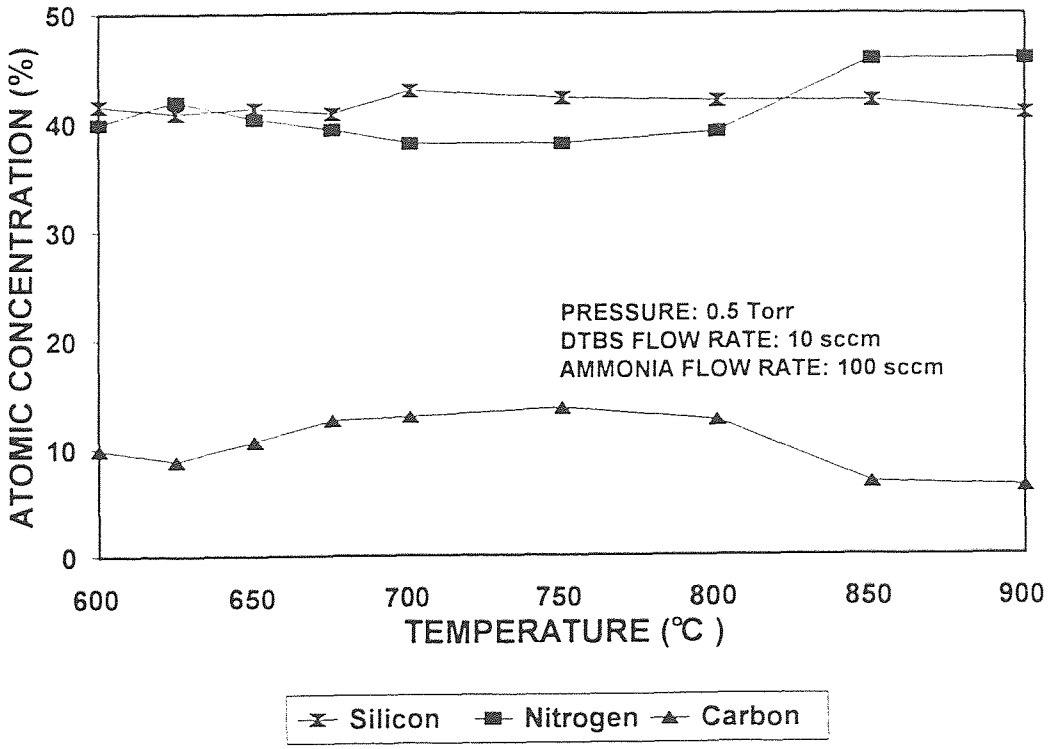

(b)

Figure 3.4 Atomic concentration of silicon nitride films as a function of deposition temperature **(a)** by RBS and **(b)** by XPS

than that possible from SiH_2Cl_2 [7, 24]. This reduced thermal processing coupled to the no apparent loss to film quality makes this process attractive to current VLSI and emerging ULSI requirements.

3.1.2 Pressure Dependent Study

The pressure dependent behavior of deposition rate is shown in figure 3.5 while the pressure dependent behavior of atomic concentration of silicon, nitrogen, and carbon is shown in figure 3.6. For a constant DTBS flow rate of 10 sccm, NH_3 flow rate of 100 sccm and temperature of 650 $^{\circ}C$, the deposition rate is found to increase over the pressure range of 0.2 to 0.8 Torr followed by a decrease of 0.8 to 1.1 Torr. As the deposition pressure increases, more gaseous reactants were adsorbed on the substrate surface and more sites were occupied by the reactant molecules. Thus, the effective reaction surface area increases, and therefore the deposition rate increases. However, as the pressure increases above 0.8 Torr, the low pumping speed is sufficient to result in the excess decomposition byproducts being adsorbed on the substrate surface and occupied more sites. The result is that the effective reaction surface area, and therefore the deposition rate, is reduced. This behavior is consistent with a Langmuir-Hinshelwood mechanism for the bimolecular surface reaction mode described in the introduction part of this thesis.

As seen in figure 3.6, stoichiometric silicon nitride films can be obtained over the entire pressure range of 0.2 to 1.1 Torr. Furthermore, though the effective substrate surface areas were different due to the different reactant-occupied sites under different pressures, the compositions of the films were stoichiometric and judiciously stable which indicates that the unanticipated decomposition products were unstable under the deposition conditions and thus were exhausted by the pumping system.

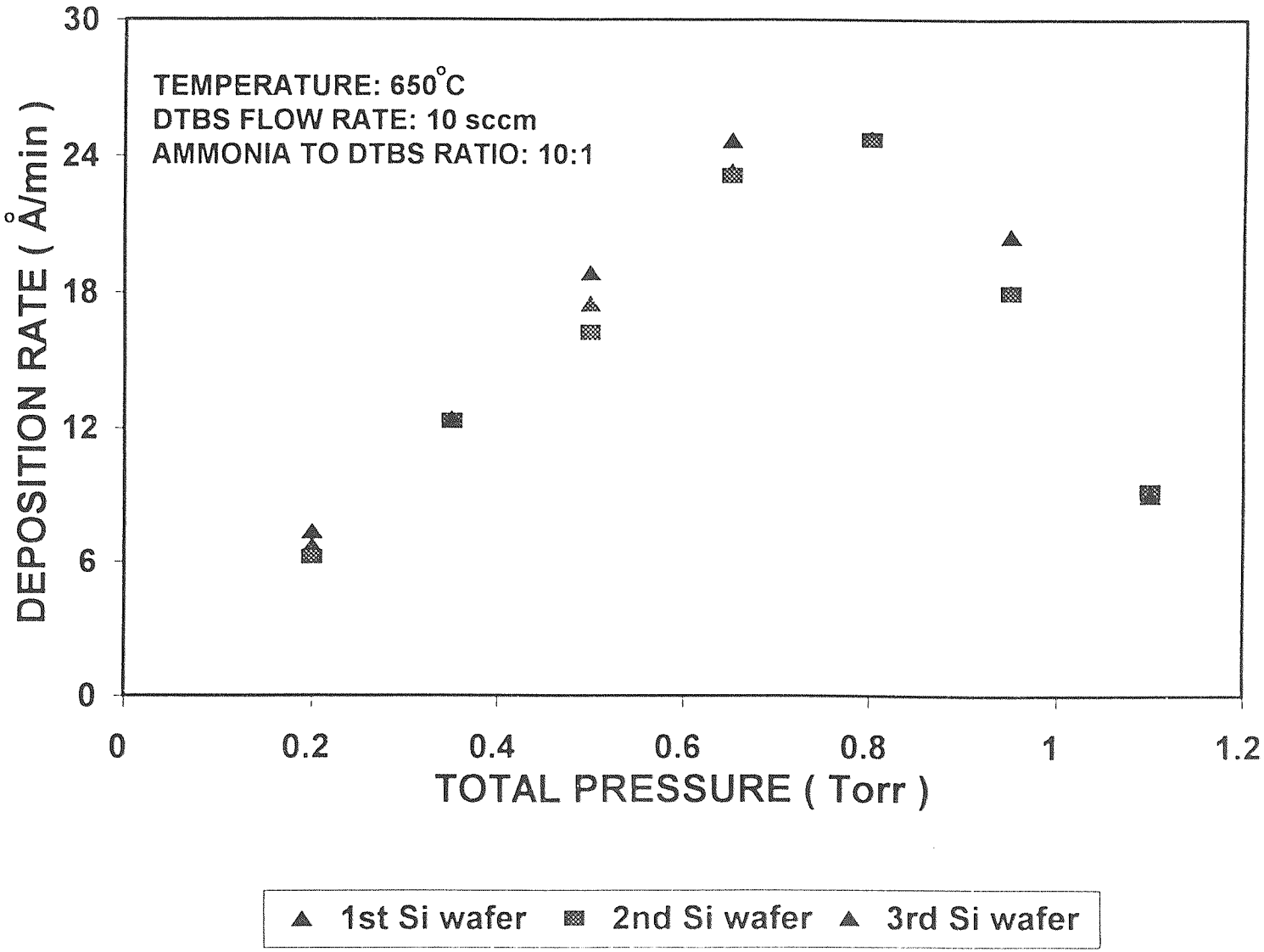

Figure 3.5 Variation of deposition rate of silicon nitride films as a function of deposition pressure

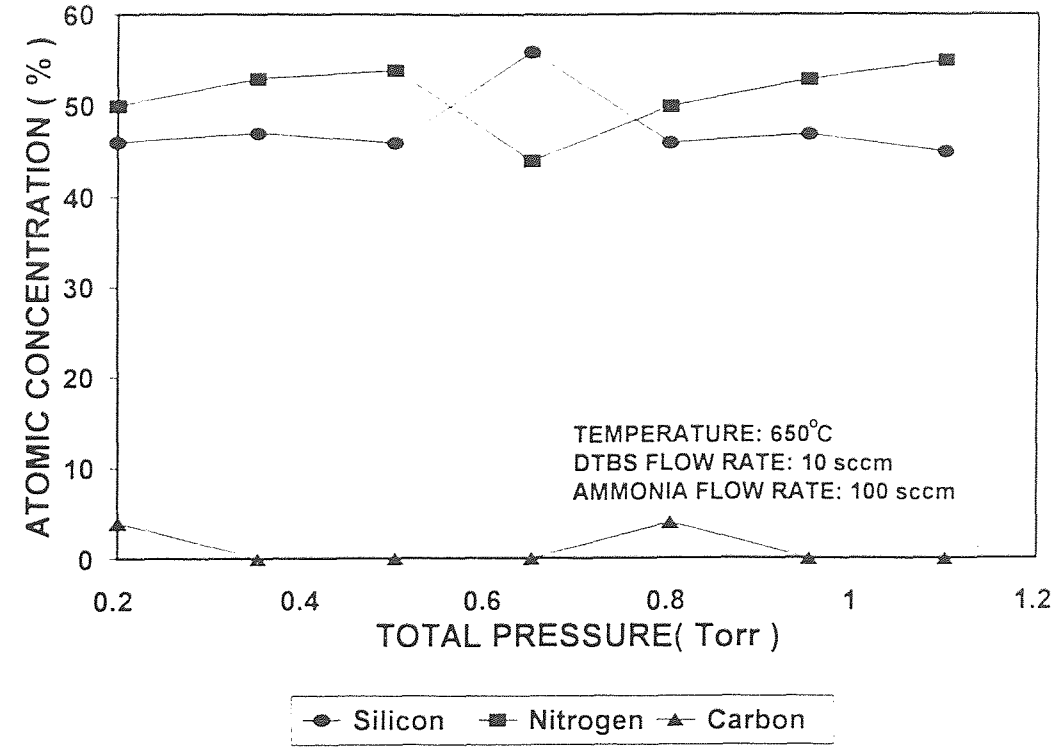

(a)

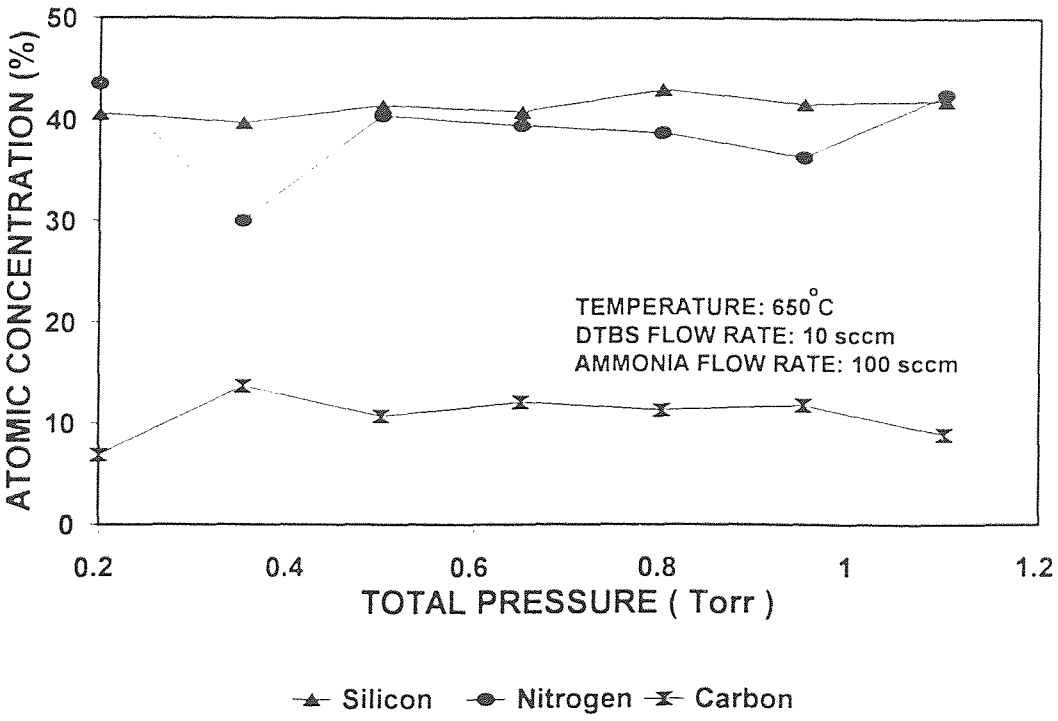

(b)

Figure 3.6 Atomic concentration of silicon nitride films as a function of deposition pressure **(a)** by RBS and **(b)** by XPS

3.1.3 DTBS Flow Rate Dependent Study

The DTBS flow rate dependent behavior of deposition rate is shown in figure 3.7 while the DTBS flow rate dependent behavior of atomic concentration of silicon, nitrogen and carbon is shown in figure 3.8. For a constant conditions of temperature (650 °C), total pressure (0.5 Torr), and NH_3/DTBS flow ratio (5), the deposition rate was found to increase monotonically with increasing DTBS flow rate over the DTBS flow rate range of 10-50 sccm. Since DTBS is one of the reactants which contributes to the formation of silicon nitride films, increasing of DTBS flow rates result in the increase of reactant molecule sites. Thus, the effective substrate surface area increases, and therefore the deposition rate increases. As seen in figure 3.8, stoichiometric and stable composition silicon nitride films can be obtained over the entire DTBS flow rate range of 10-50 sccm which reflects the exhaust of gaseous byproducts by the pumping system.

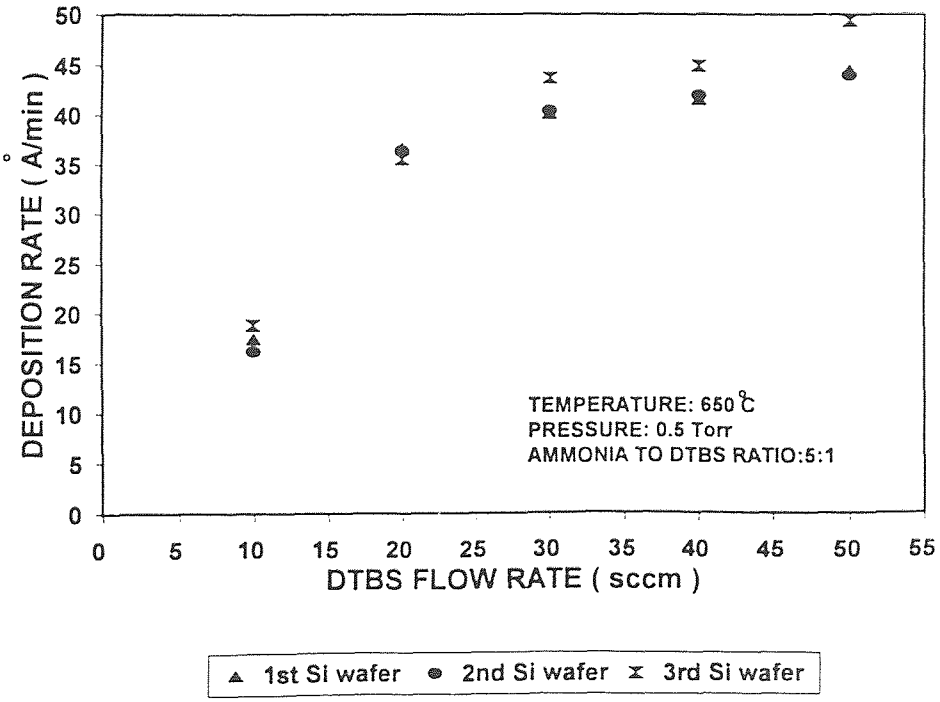

Figure 3.7 Variation of deposition rate of silicon nitride films as a function of DTBS flow rate

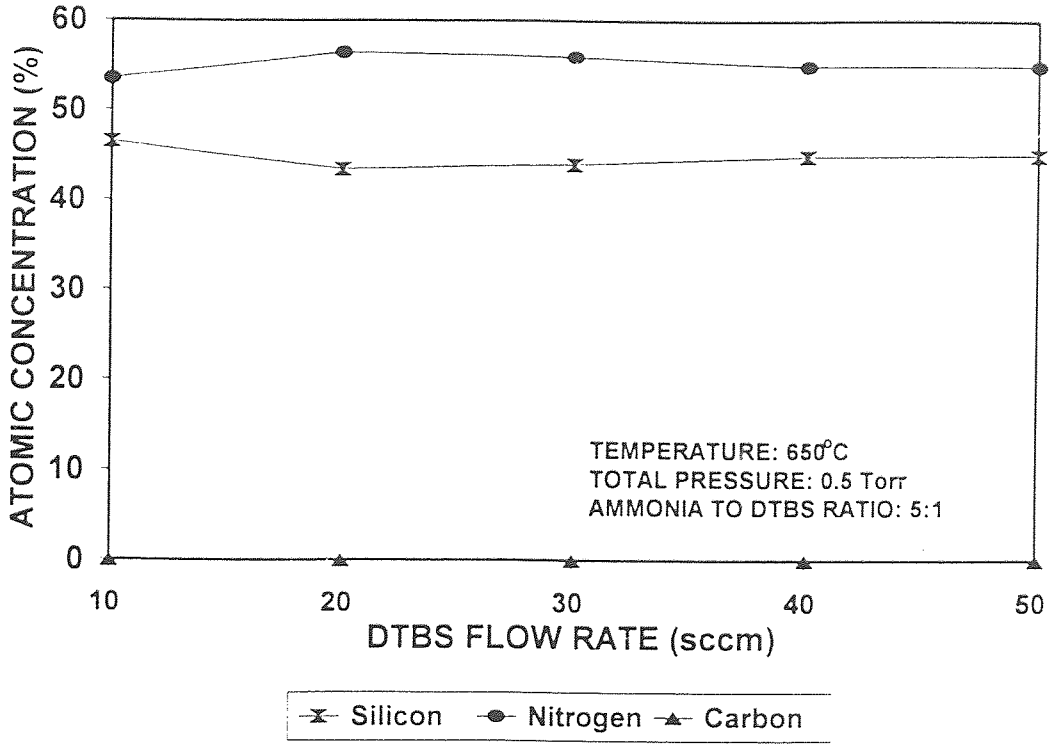

(a)

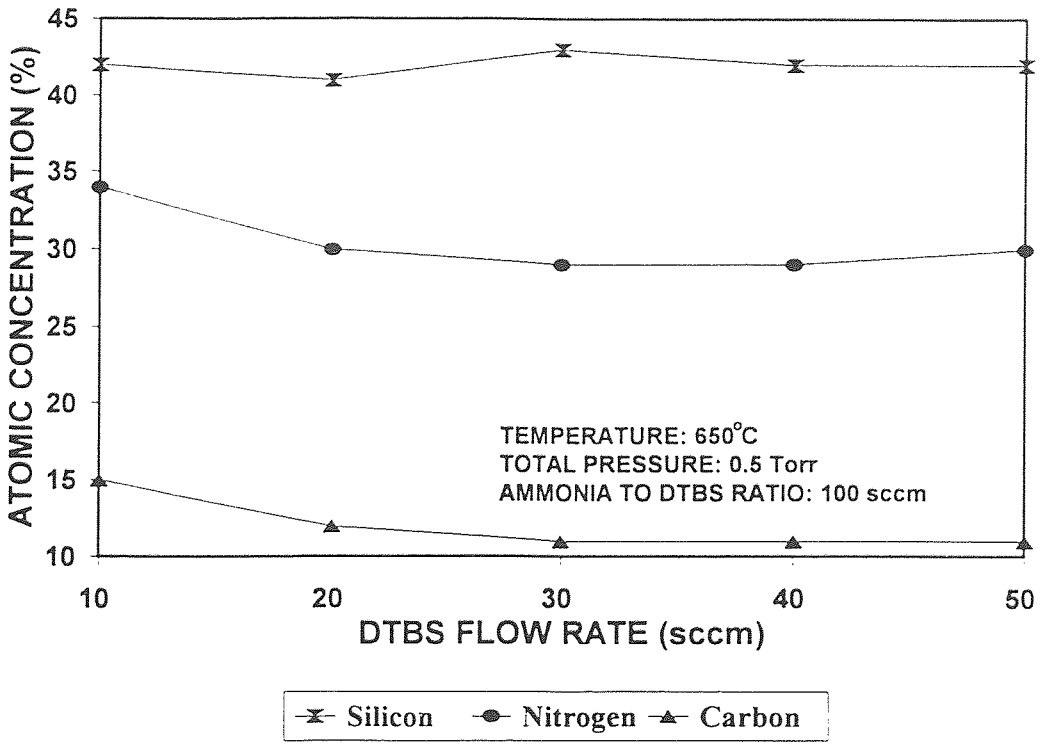

(b)

Figure 3.8 Atomic concentration of silicon nitride films as a function of DTBS flow rate **(a)** by RBS and **(b)** by XPS

3.1.4 NH_3/DTBS Flow Ratio Dependent Study

In this series of experiments, NH_3/DTBS ratio was varied from 5 to 25 for constant conditions of temperature (650 °C), DTBS flow rate (10 sccm), and total pressure (0.5 Torr). In figure 3.9, the deposition rate is plotted as a function of the square root of NH_3/DTBS flow ratio. It can be seen from this plot that as the NH_3/DTBS flow ratio increases, the deposition rate decreases rapidly. This phenomenon can be explained by considering the diluting effect of NH_3. When the flow rate ratio increases as the NH_3 flow rate is increasing, the constant total pressure of 0.5 Torr is maintained by increasing the pumping speed which in turn causes a reduction in the precursor partial pressure.

The observed linear dependence on the square root of NH_3/DTBS flow ratio had been observed previously [41] and can be explained by recognizing that a laminar flow in the annular region can affect the partial pressure of NH_3 in the interwafer region. As the total flow rate in the annular region increases with increasing NH_3/DTBS flow ratio, the pumping rate in this region must increase accordingly in order to maintain the desired constant pressure. Such action is expected to facilitate by-product removal rate and result in an increasing partial pressure of reactant gas in the interwafer region until a maximum concentration is approached.

Figure 3.10 illustrates the atomic concentration of silicon, nitrogen, carbon as a function of NH_3/DTBS flow ratio. As seen in this figure, stoichiometric and stable compositions of silicon nitride films can be obtained over the entire NH_3/DTBS flow ratio range of 5-25 which indicates that the decomposition byproducts are either unstable or gaseous and thus were exhausted by the pumping systems.

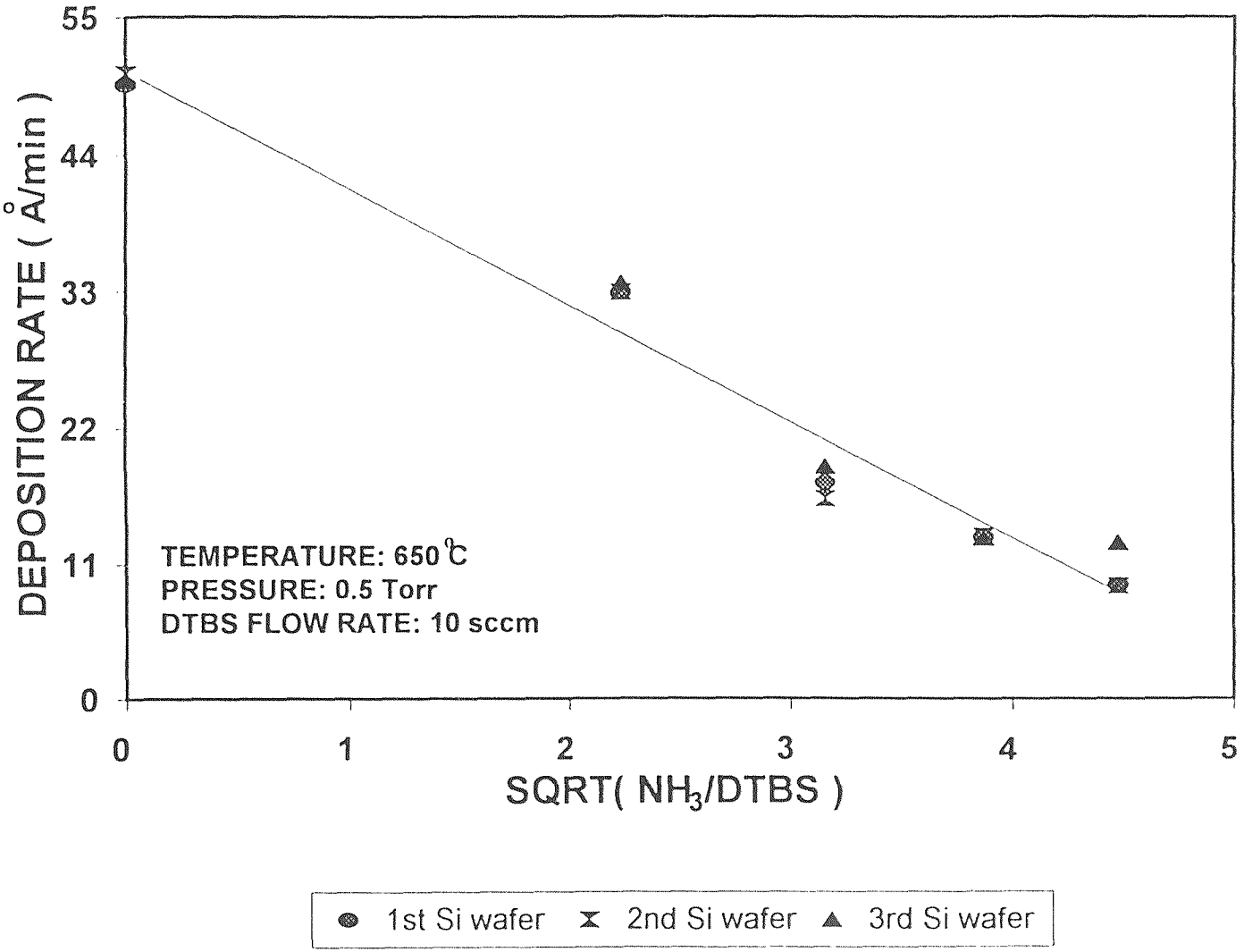

Figure 3.9 Variation of deposition rate of silicon nitride films as a function of the square root of NH_3/DTBS flow ratio

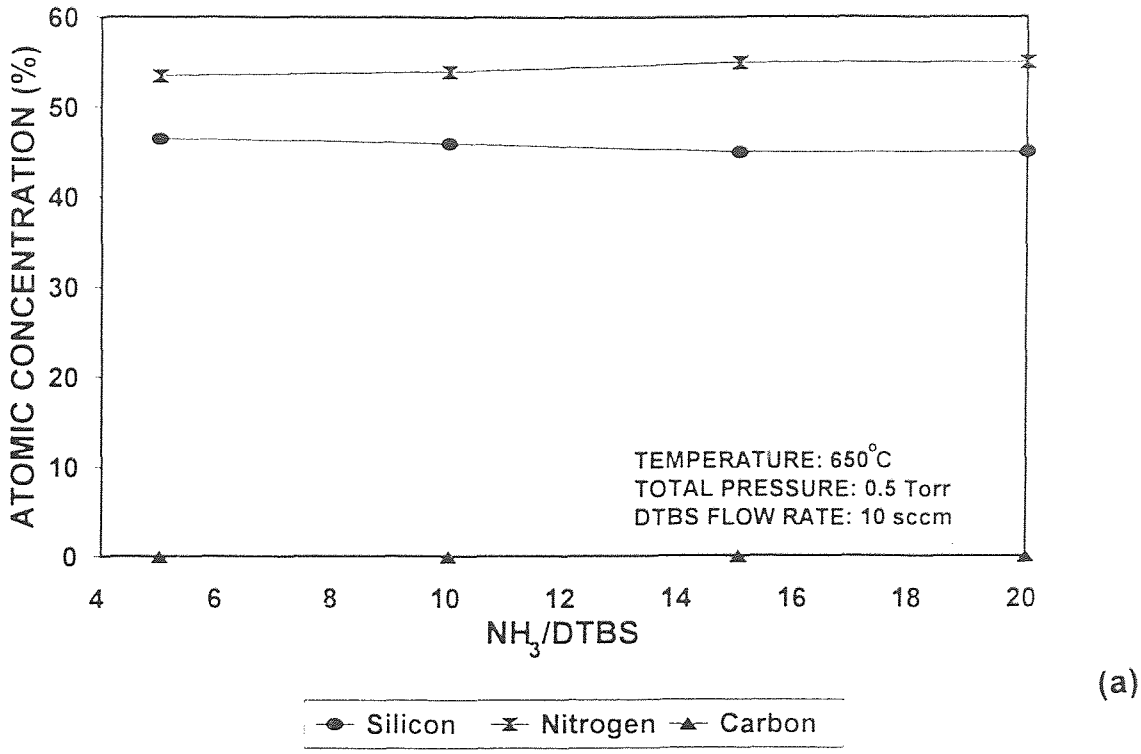

(a)

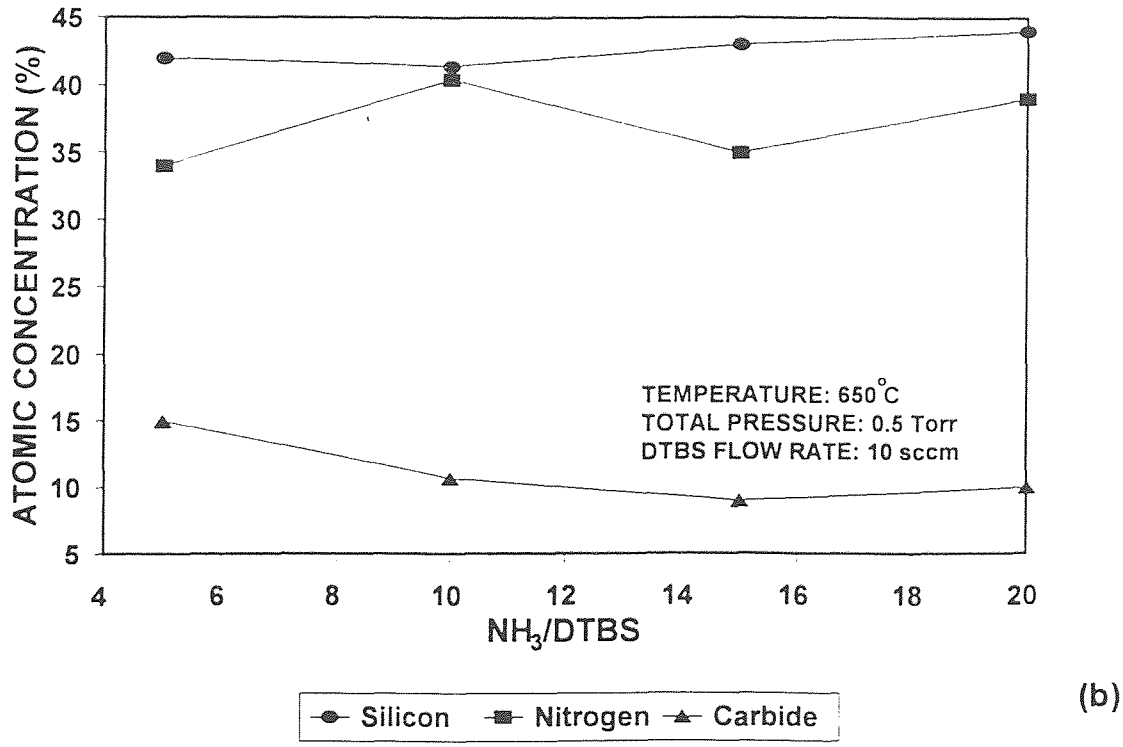

(b)

Figure 3.10 Atomic concentration of silicon nitride films as a function NH_3/DTBS flow ratio **(a)** by RBS and **(b)** by XPS

3.2 Silicon Nitride Film Characterizations

3.2.1 Density

A graph plotted by taking thickness of the films deposited at different temperatures and deposition times, against weight gain on the same wafer, is shown in figure 3.11. The thickness of the film deposited on one side was measured at five different points and the average film thickness calculated. From the slope of the observed linear dependence, the density of the as-deposited silicon nitride films was calculated to be equal to 2.74 g/cm^3 from the mass-volume relationship :

$$D = \frac{\Delta W}{A * T} \qquad (4.1)$$

where ΔW is the weight gain due to deposition on the Si wafer, A is the wafer surface area and T is the thickness of the film. Regression analysis was carried out for that plot and the extrapolated points in the curve were well within one standard deviation.

The calculated density value is a little lower than the reported value of 2.9 to 3.1 g/cm^3 for silicon nitride[18]. This may be accounted for by the pin holes of the films and the amorphous nature of the deposits. The X-ray diffraction patterns show that the films were amorphous even at the highest deposition temperature of 900 °C. as seen in figure 3.12.

3.2.2 Uniformity and Optical Microscopic Observation of Films

The deposited silicon nitride films appear smooth and uniform which is consistent with the small measured film thickness variation and the observed microstructure property. The optical microscopic observation of the deposited silicon nitride film shows that the films deposited over the temperature range of 600 to 675 °C have no gas phase nucleation and better microscopical

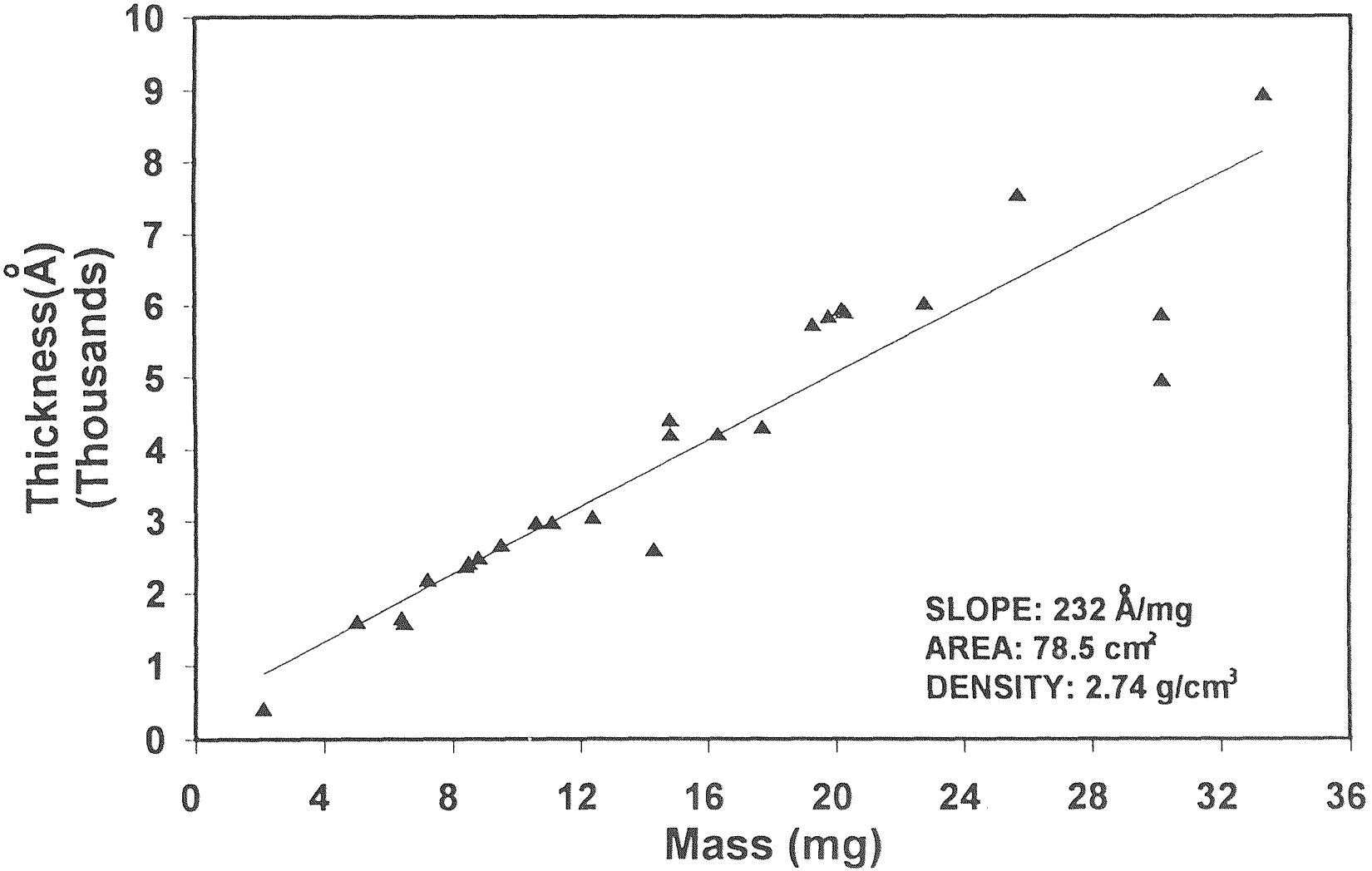

Figure 3.11 A plot of average film thickness versus weight gain on the wafer for silicon nitride films

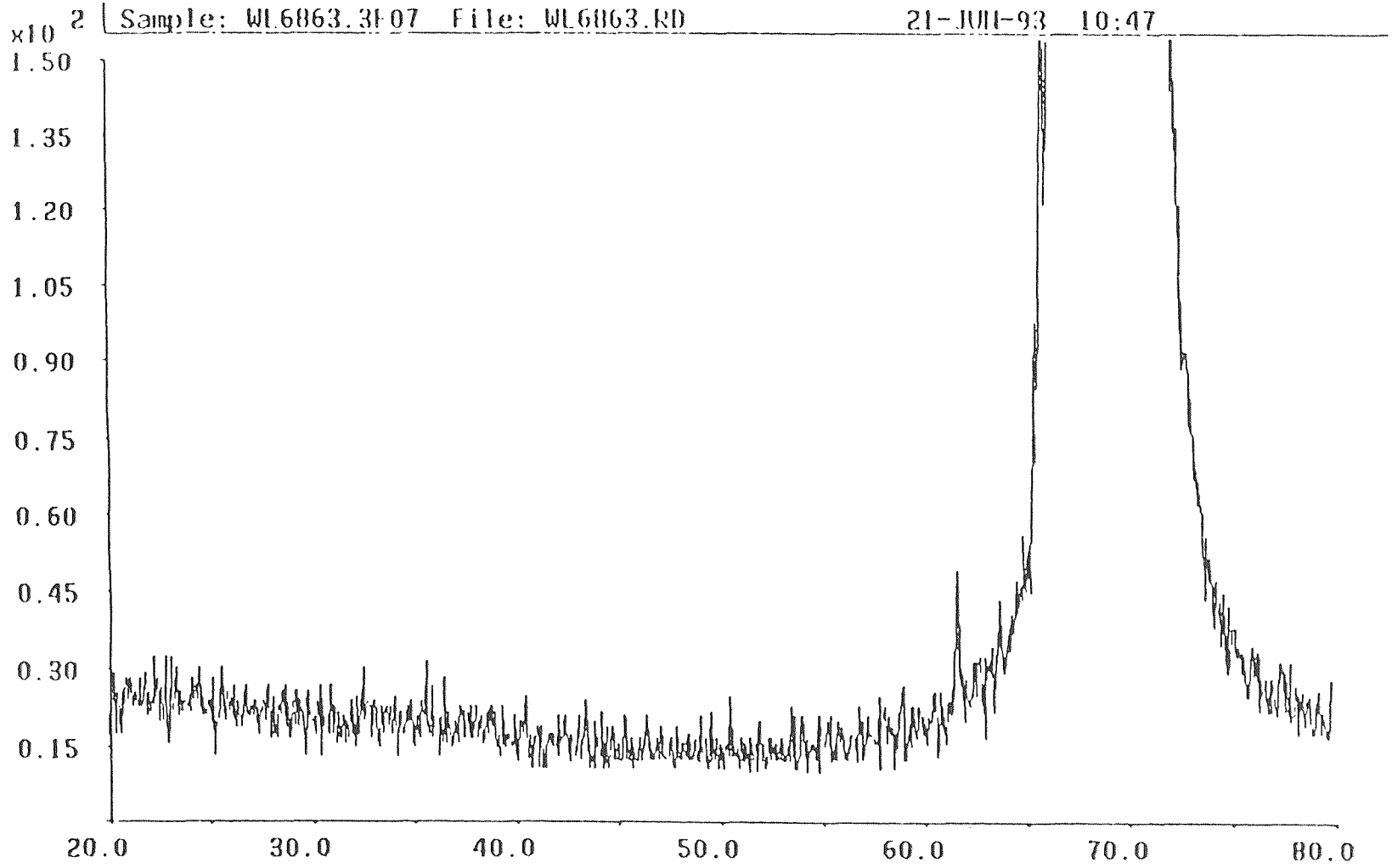

Figure 3.12 X-ray diffraction pattern for a silicon nitride film on silicon deposited at a temperature of 900 °C, pressure of 0.5 Torr, DTBS flow rate of 10 sccm, and NH_3 flow rate of 100 sccm

smoothness which coincides with the surface reaction rate limited regime. Films deposited in this regime with appropriate deposition rate (about 25 Å/min) exhibit extremely good uniformity under optical microscopic observation.

No microcracks were found for films thinner than 4000 Å. However, for films thicker than 4000 Å, microcracks were observed to follow parallel patterns accounting for stress release along <111> and <110> planes on the silicon substrates.

3.2.3 FTIR Analysis

FTIR spectra were gathered for all silicon nitride deposits to inspect for the presence of different vibrational modes. The results shown in figure 3.13 for a film deposited at 900 °C. reveal a peak at 870 cm^{-1} that corresponds to the standard Si-N vibrational mode. and peaks located at 3340 cm^{-1} and 2170 cm^{-1} that correspond to the N-H and Si-H vibrational modes, respectively. Previous work showed that LPCVD silicon nitride films synthesized from SiH_2Cl_2 and NH_3 precursor systems failed to reveal the Si-H and N-H bonds above 800 °C [23,41]. The reason is that Si-H and N-H bounds tend to decompose at the higher temperature.

3.2.4. Refractive Index

The dependence of refractive index on temperature, pressure, DTBS flow rate and NH_3/DTBS flow ratio have been investigated. It can be seen from figure 3.14 that the refractive index value increases slightly from 1.93 to 2.2 with higher temperature. Figure 3.15 illustrates the dependency of refractive index of deposited silicon nitride films on deposition pressure, but it was difficult to extract information from that dependency. No significant variation in the refractive index was noted when the DTBS flow rate and NH_3/DTBS flow ratio

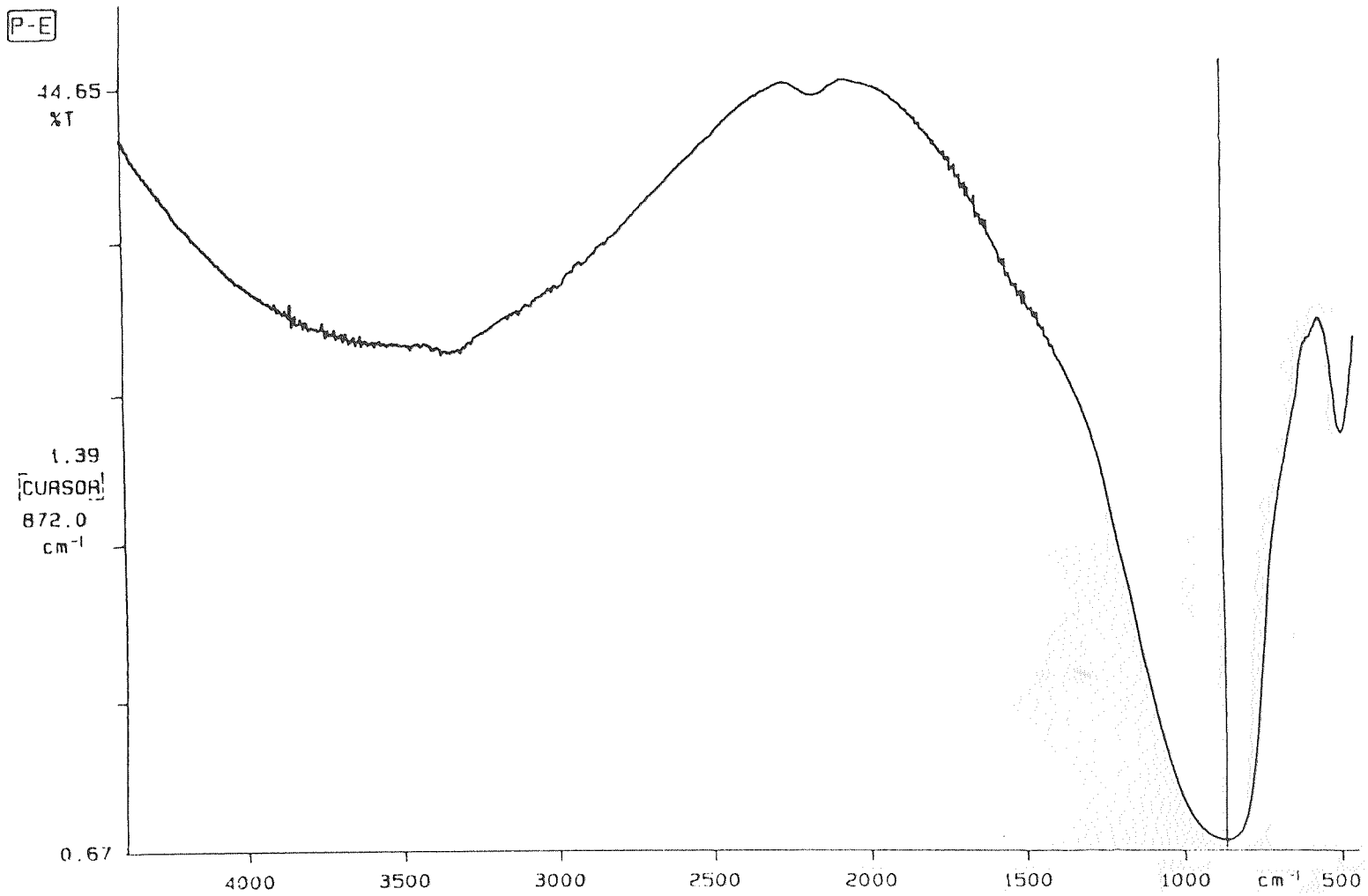

Figure 3.13 FTIR spectrum for a silicon nitride film on a silicon substrate deposited at a temperature of 900 °C, pressure of 0.5 Torr, DTBS flow rate of 10 sccm, and NH_3 flow rate of 100 sccm

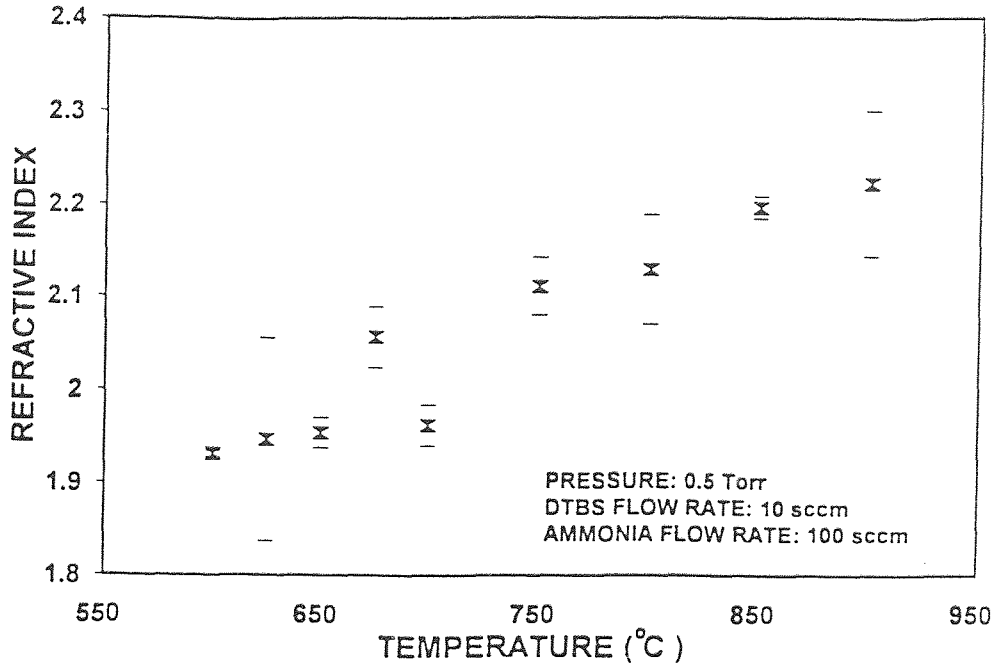

Figure 3.14 Effect of deposition temperature on refractive index of silicon nitride films

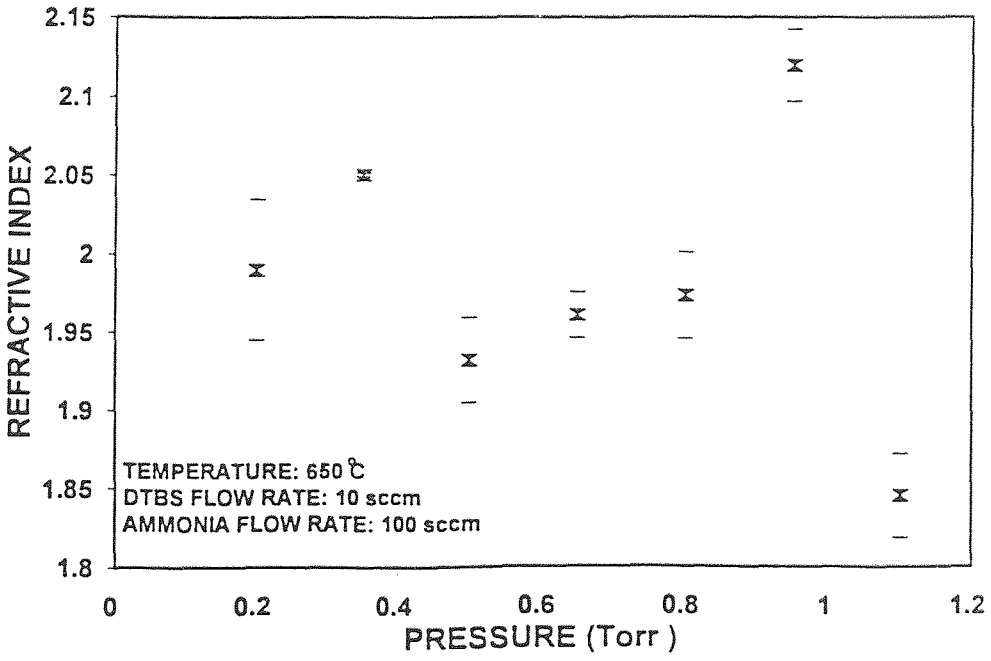

Figure 3.15 Effect of deposition pressure on refractive index of silicon nitride films

were varied (figures 3.16 and 3.17).

In general, the refractive index value of all the deposited silicon nitride films show no systematic variations. All the refractive index values of these films are in the range of 1.8 to 2.2. Among them, most samples have refractive index values between 1.9 and 2.1 which reflects the stoichiometric composition of as-deposited silicon nitride films. The only abrupt increase of the refractive index value found in figure 3.17 is due to the absence of NH_3 in deposition which results in typical silicon carbide films with refractive index value near 2.7. This result was also confirmed by the compositional analysis of the films by RBS and XPS Analyses.

It can be concluded from these analyses that the LPCVD silicon nitride films from DTBS/NH_3 precursor system have systematic and standard refractive index values which reflects the stoichiometric composition of the deposited silicon nitride films. This conclusion is also correlates with the compositional analyses described in section 3.1.

3.2.5 Optical Properties

The optical transmission and absorption coefficient of silicon nitride films deposited on fused quartz wafers were obtained from UV Visible measurement results in the ultraviolet-visible region (200 -800 nm wavelength) and the absorption coefficients have been calculated for a wavelength of 633 nm which was considered to represent the absorption in the visible region.

According to Beer's law, optical transmission

$$\% T = \frac{I}{I_o} = e^{-\alpha t} \qquad (4.2)$$

where α is the absorption coefficient, I is the radiation intensity and t is the

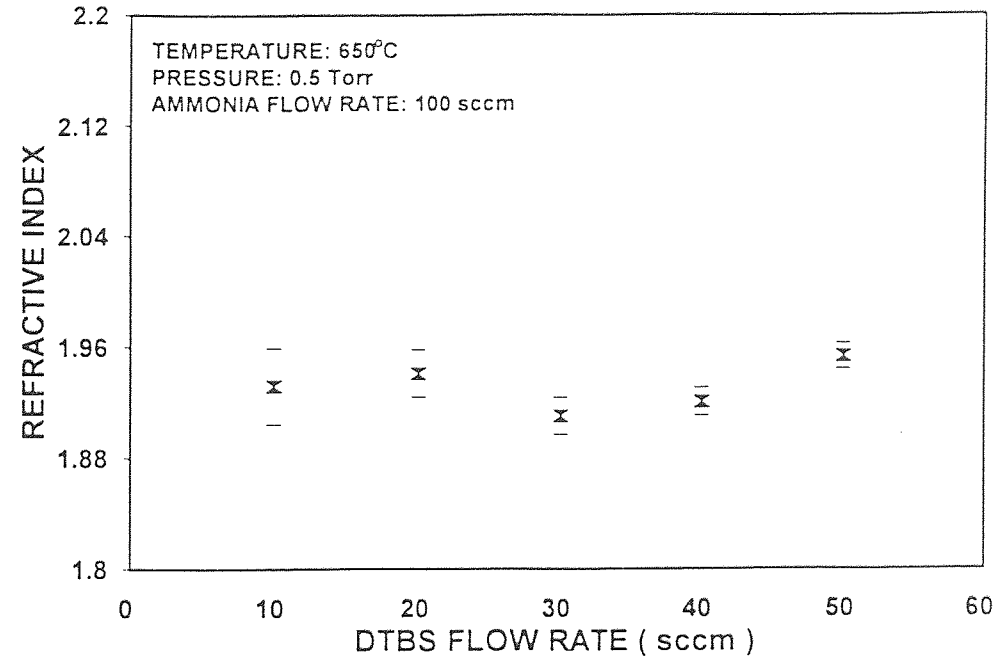

Figure 3.16 Effect of DTBS flow rate on refractive index of silicon nitride films

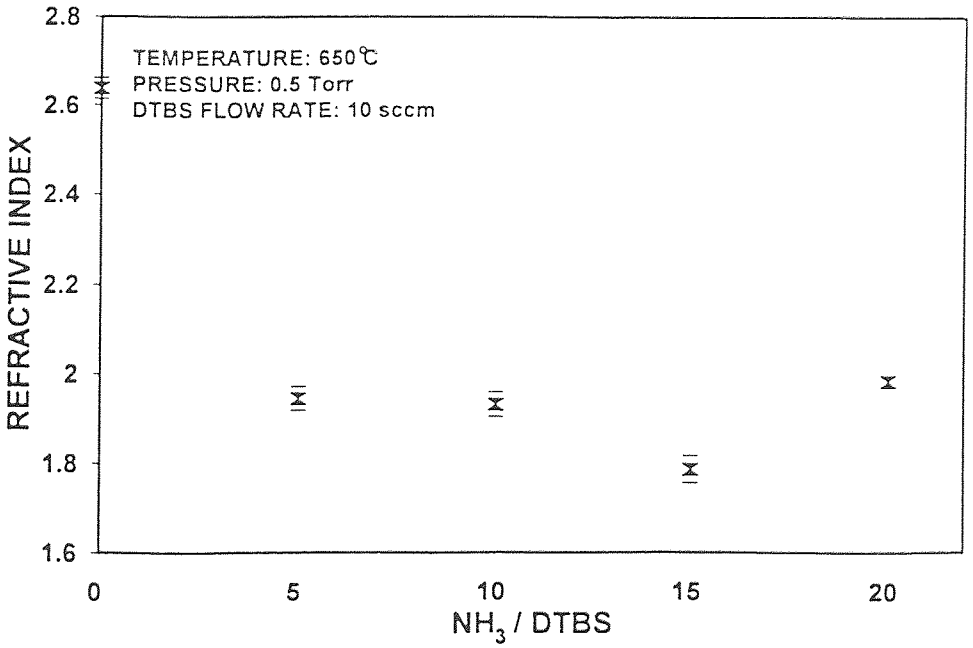

Figure 3.17 Effect of NH_3/DTBS flow ratio on refractive index of silicon nitride films

thickness of the film. By determining the optical transmission $I/I_{o,}$, then calculating the thickness of the UV visible sample (quartz wafer) from the film weight and the pre-calculated film density on the silicon sample from the same run, thereby the absorption coefficient of the film can be obtained from eq.4.2. As shown in figure3.18, the percent transmission I/Io was determined by the midpoint of the schematically maximum and minimum transmission curve at 633 nm.

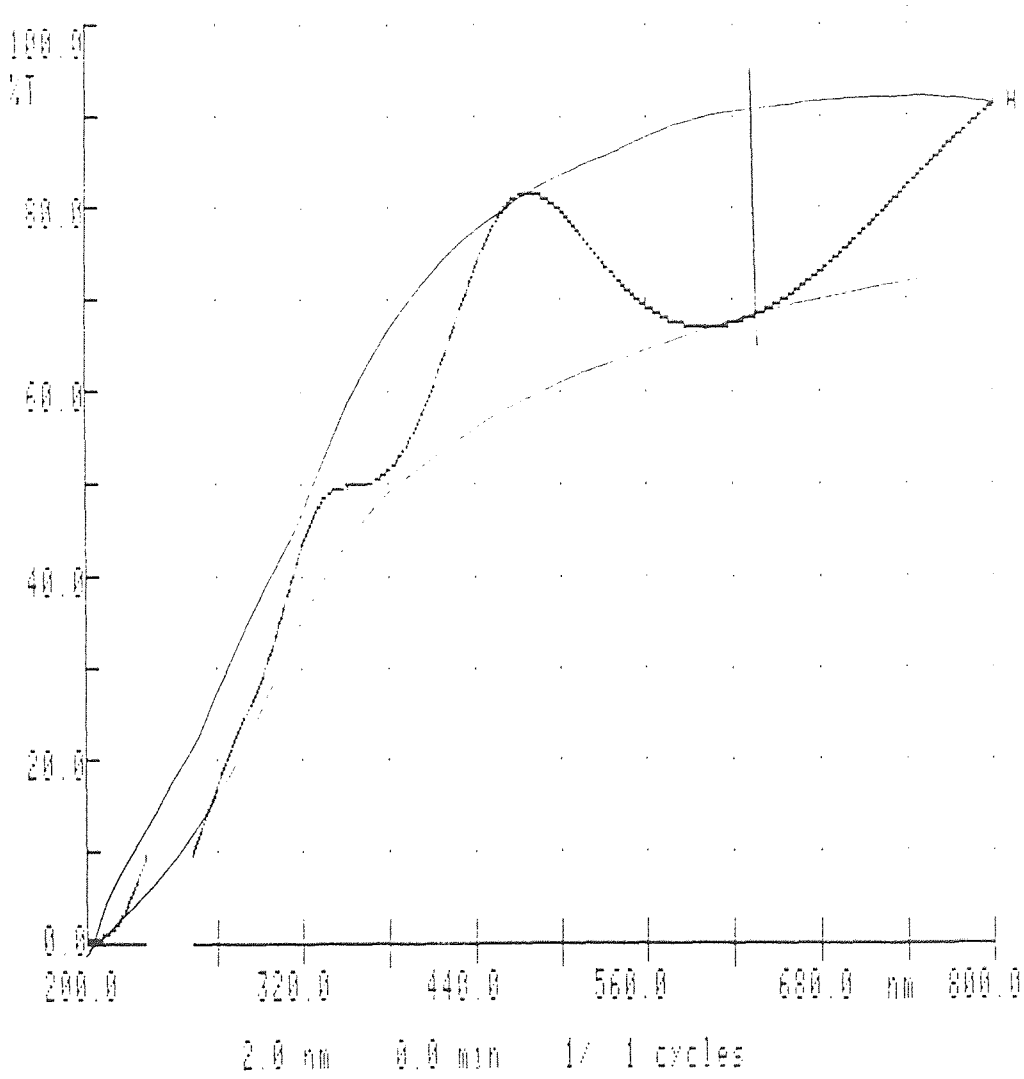

Figure 3.18 Determination of I/Io from UV Visible measurements

Figures 3.19 and 3.20 illustrates the variations of optical transmission normalized to 1μm silicon nitride films as functions of deposition temperature and pressure respectively.

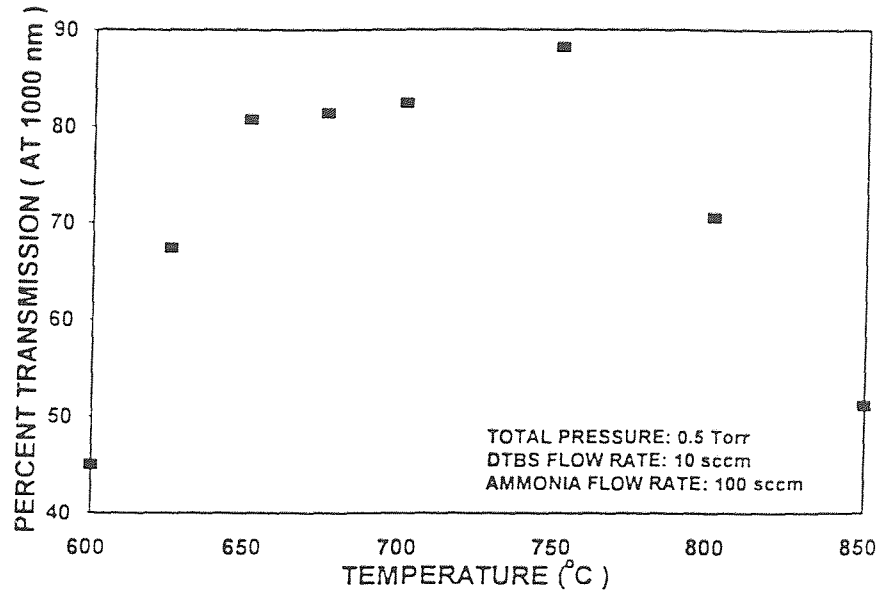

Figure 3.19 Variation of optical transmission of silicon nitride films normalized to 1 μm thick silicon nitride film as a function of deposition temperature.

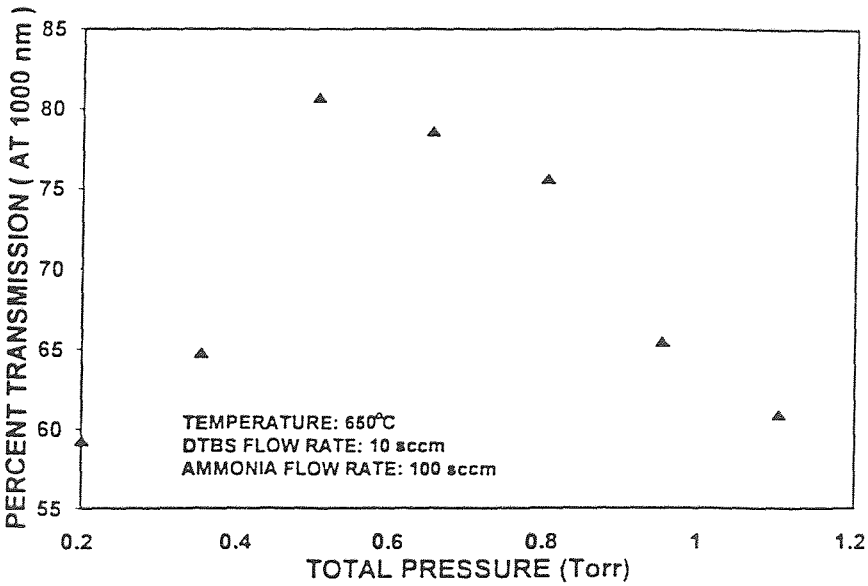

Figure 3.20 Variation of optical transmission of silicon nitride films normalized to 1 μm thick silicon nitride film as a function of deposition pressure.

3.2.6 Mechanical Properties

The stress values of all the one side deposited stress wafers show that all the LPCVD silicon nitride films from DTBS/NH_3 precursor system are tensile.

The hardness and Young's modulus of as-deposited silicon nitride films were measured with Nano Instruments Indenter. Figures 3.21 and 3.22 illustrate the variations of hardness as a function of deposition temperature and pressure while figures 3.23 and 3.24 represent the variations of Young's modulus as a function of deposition temperature and total pressure. It can be concluded from these figures that both hardness and Young's modulus increase with the increasing temperature. As to the influences of total pressure on hardness and Young's modulus, there were no rules to follow.

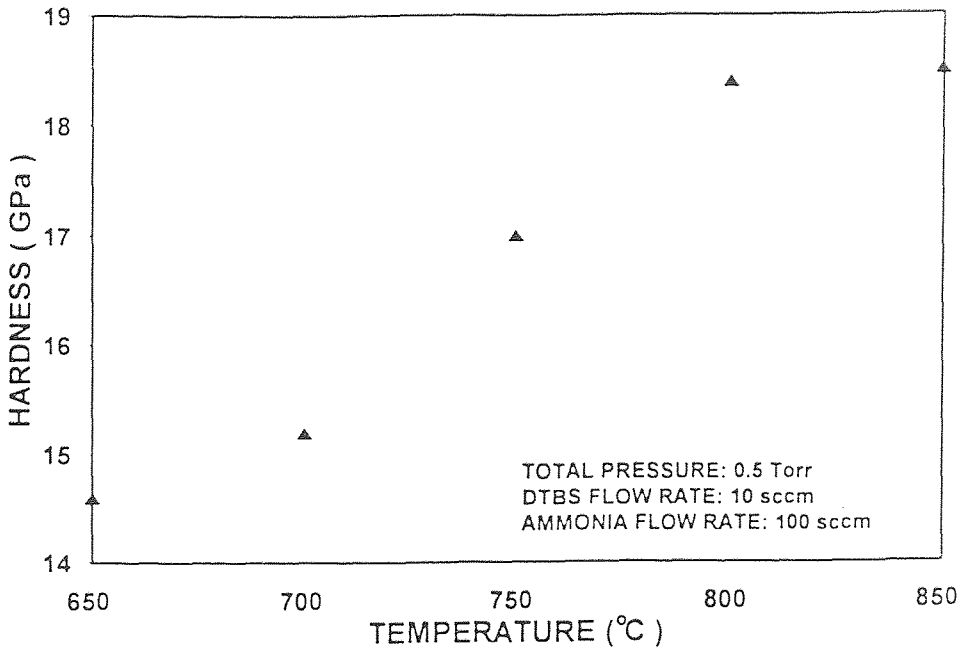

Figure 3.21 Variation of hardness of silicon nitride films as a function of deposition temperature.

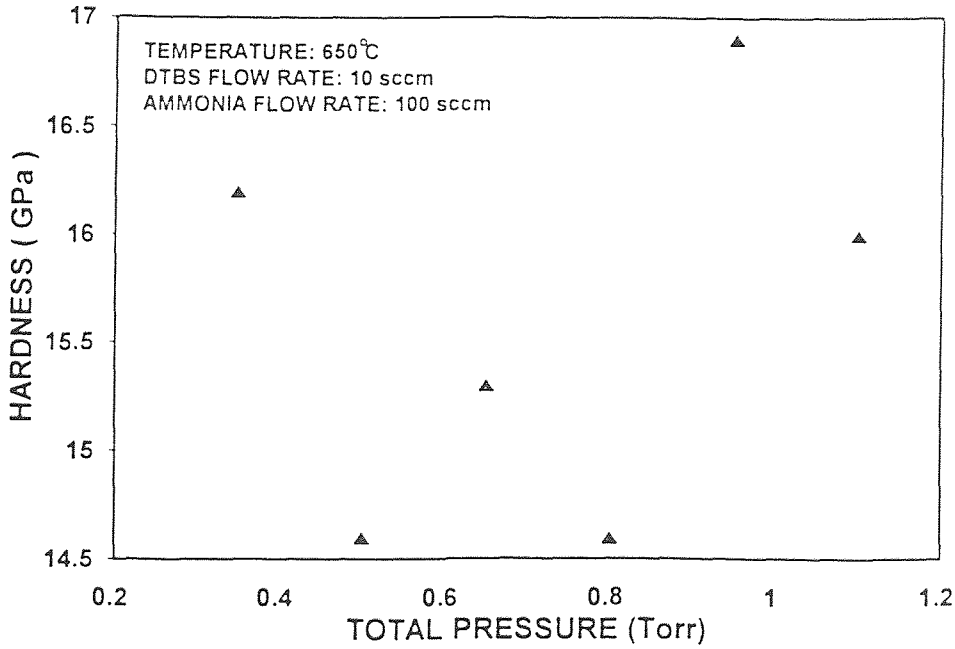

Figure 3.22 Variation of hardness of silicon nitride films as a function of deposition pressure.

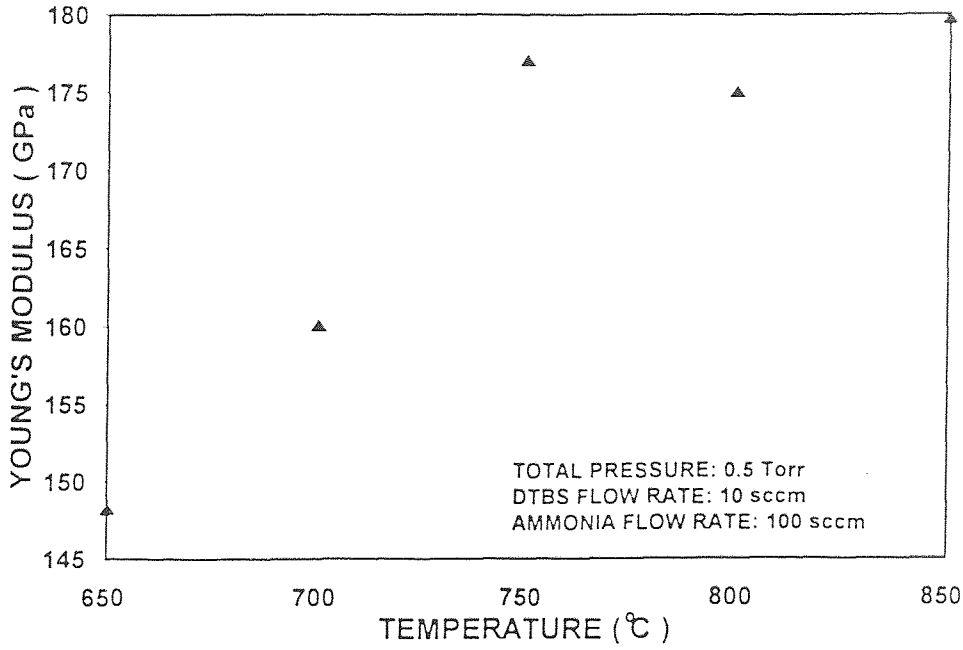

Figure 3.23 Variation of Young's modulus of silicon nitride films as a function of deposition temperature.

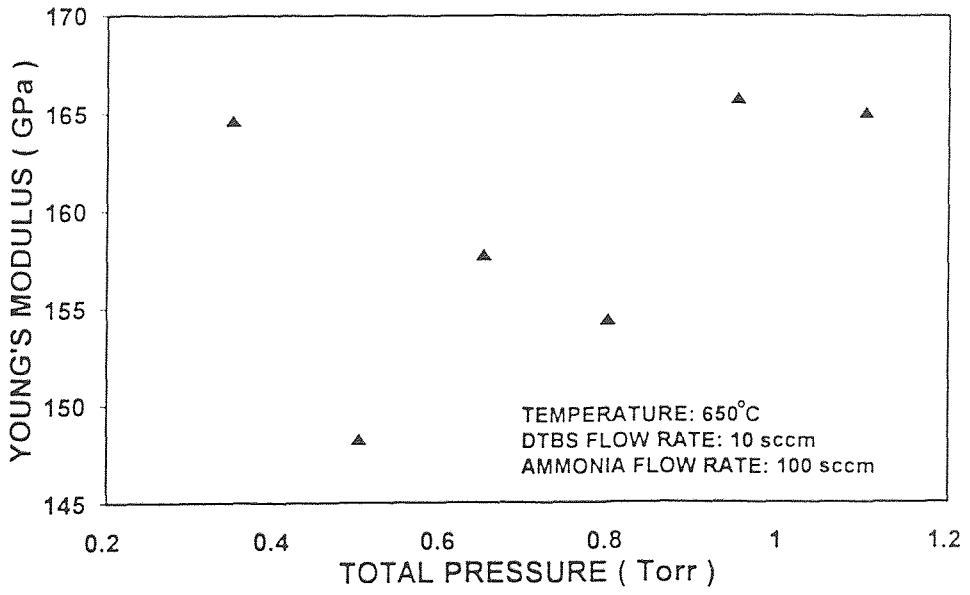

Figure 3.24 Variation of Young's modulus of silicon nitride films as a function of deposition pressure.

CHAPTER 4

CONCLUSIONS

Amorphous high quality stoichiometric Si_3N_4 films had successfully been synthesized on silicon and quartz wafers by low pressure chemical vapor deposition from DTBS/NH_3 precusor system in the temperature range of 600- 900 °C, pressure range of 0.2- 1.1 Torr, DTBS flow rate range of 10-50 sccm and NH_3/DTBS flow ratio range of 5-25. The feasibility of using DTBS in LPCVD silicon nitride films had been demonstrated through the kinetics studies and film characterization studies. The temperature dependent behavior of deposition rate was found to follow an Arrhenius behavior in the temperature range of 600 to 700 °C with an activation energy of 50.0±0.2 kcal/mol. The pressure dependent behavior of deposition rate was found to follow a bimolecular surface reaction mode. The X-ray diffraction patterns indicate the amorphous nature of as-deposited silicon nitride films. FTIR spectra reveals the expected presence of the Si-N vibrational mode near 840cm^{-1}. The refractive index values are between 1.9 - 2.1 indicating stoichiometric silicon nitride film compositions which was corroborated by film compositional analyses from RBS and XPS. All the films are tensile. Hardness and Young's modulus of as-deposited films were found to increase with increasing temperature.

Furthermore, through the film growth kinetics studies and film characterization study, an optimum film synthesis condition was found to be under the temperature of 650 °C, total pressure of 0.65 Torr, DTBS flow rate of 10 sccm, and NH_3/DTBS flow ratio of 5:1.

REFERENCE

1. Blaauw, C. "Preparation and Characterization of Plasma-Deposited Silicon Nitride." *J. Electrochem. Soc.* 131 (May 1984): 1114-1118

2. Morosanu, C.-E. "The Preparation, Characterization and Applications of Silicon Nitride Thin Films." *Thin Solid Films* 65 (1980): 171-208

3. Frieser, R. G. "Direct Nitridation of Silicon Substrates." *J. Electrochem. Soc.* 115 (Oct. 1968): 1092-1094

4. Mitchell, J. B., P. P. Pronko, J. Shewchun, and D. A. Thompson. "Nitrogen-implanted silicon. I. Damage Annealing and Lattice Location." *J. Appl. Phys.* 46 (1975): 332-334

5. Wada, Y., and M. Ashikawa. "Silicon Planner Devices Using Nitrogen Ion Implantation." *Jpn. J. Appl. Phys.* 15 (1975): 1725-1730

6. Van den brekel, C. H. J. "Chemical Vapor Deposition." *J. M. Blocher, G. E. Vuilland, and G. Wahl Eds., The Electrochemical Society, Pennington, New Jersey, U. S. A.* (1981): 116

7. Kern, W. "Chemical Vapor Deposition." *R. A. Levy Eds., Microelectronic Materials and Processes. Kluwer Academic, New Jersey, U.S.A.* (1986): 203-246

8. Kern, W., and V. Ban. "Chemical Vapor Deposition of Inorganic Thin Films." *J. L. Vossen, and W. Kern Eds., Thin Film Processes. Academic, New York, U. S. A.* (1978): 257-331

9. Claassen, W. A. P., J. Bloem, W. Q. J. N. Valkenburg and C. H. J. Van den brekel. "The Deposition of Silicon from silane in a Low-pressure Hot-wall System." *J. Crystal Growth.* 57 (1982): 259-266

10. Laidler, K. J. *Chemical Kinetics. Harper & Row , New York, U. S. A.* (1987): 267-276

11. O'Mara, W. C., R. B. Herring, L. P. Hunt. *Handbook of Semiconductor Silicon Technology. Noyes Publications, New Jersey, U. S. A.* (1990): 644

12. Hammond, M. "Intro. to Chemical Vapor Deposition." *Solid State Technol.* 63 (Dec. 1979): 61

13. Kern. W., and G. L. Schnable. " Low Pressure Chemical Vapor Deposition for Very Largy Scale Integration Processing---A Review." I*EEE Trans. Electron Devices.* ED-26 (1979): 647-657

14. Rosler, R. S. "Low Pressure CVD Production Processes for Poly, Nitride, and Oxide." *Solid State Technol.* (April 1977): 63-70

15. Tanikawa, E., T. Okabe, and K. Maeda. "Doped Oxide Films by Chemical Vapor Deposition." *G. F. Wakefield, and J. M. Blocher Eds. The Electrochemical Soc. Princeton, New Jersey, U. S. A.* (1973): 261-274

16. Stering, H. F., and R. C. G. Swann. "Chemical Vapor Deposition Promoted by r.f.Discharge." *Solid State Electronics.* 8 (1965): 653-654

17. Woodward, J., D. C. Cameron, L. D. Irving, and G. R. Jones. "The Deposition of Insulators onto InP using Plasma-Enhanced Chemical Vapor Deposition." *Thin Solid Film.* 85 (1981): 61

18. Sze, S. M. *VLSI Technology. McGraw-Hill, New York, U. S. A.* (1988): 233-269

19. Van de ven, E. P. G. T. "Plasma Deposition of Silicon Dioxide and Silicon Nitride Films." *Solid State Technol.* 24 (1981): 167-171

20. Pan, P., and W. Berry. " The Composition and Physical Properties of LPCVD Silicon Nitride Deposited with Different NH_3/SiH_2Cl_2 Gas Ratios." *J. Electrochem. Soc.* 132 (Dec. 1985): 3001

21. Petroff, P. M., G. A. Rozgonyi, and T. T. Sheng. "Elimination of Process-Induced Stacking Faults by Preoxidation Getterings of Si Wafers: II Si_3N_4 Process." *J. Electrochem. Soc.* 123 (1976):565-570

22. Katoh, K., M. Yasui, and H. Watanabe. "Plasma Enhanced Deposition of Silicon Nitride from SiH_4-N_2 Mixture." *Jap. J. Appl. Phys.* 22 (1983): L321-323

23. Habraken, F. H. P. M., R. H. G. Tijhaar, W. F. van der Weg, A. E. T. Kuiper and M. F. C. Willemsen. "Hydrogen in Low-pressure Chemical-vapor-deposited silicon (oxy)nitride films." *J. Appl. Phys. 59(2)* (Jan. 1986): 447-453

24. Sze, S. M. *Semiconductor Devices Physics and Technology. John Wiely & Sons, New York, U. S. A.* (1985): 360

25. Hezel, R., and R. Schorner. "Plasma Silicon Nitride--A Promising Dielectric to Achieve High-quality Silicon MIS/IL Solar Cells." *J. Appl. Phys.*52 (1981): 3076-3079

26. Watanabe, H., K. Katoh, and M. Yasui. "Effects of rf Power and Substrate Temp. on Properties of a-SiN_x:H Films Prepared by Glow-Discharge of SiH_4-N_2-H_2." *Jap. J. Appl. Phys.* 23 (1984): 1-5

27. Soller, B. R., C. R. Snider, and R. F. Shuman. "A Flexible Multilayer Resist System Using Low Temperature Plasma-Deposited Silicon Nitride." *J. Electrochem. Soc.* 131 (1984): 868-872

28. Suzuki, K., J. Matsui, and T. Torikai. "SiN membrane Masks for X-ray Lithography." *J. Vac. Sci. Tech.* 20 (1982): 191-194

29. Doo, V. Y., D. R. Nichols, and G. A. Silvey. "Preparation and Properties of Pyrolytic Silicon Nitride." *J. Electrochem. Soc.* 113 (1966): 1279-1281

30. Kenneth, E. B., P. Glein, and R. L. Yeakley. "Some Properties of Vapor Deposited Silicon Nitride Films Using the SiH_4-NH_3-H_2 System." *J. Electrochem. Soc.* 114 (1967): 733-737

31. Grieco, M. J., F. L. Worthing, and B. Schwartz. "Silicon Nitride Thin Films from $SiCl_4$ plus NH_3: Preparation and Properties." *J. Electrochem. Soc.* 11 (may 1968): 525-531

32. Wohlheiter, V. D., and R. A. Whitner. "A High Production System for the Deposition of Silicon Nitride." *J. Electrochem. Soc.* 119 (1972): 945-948

33. Roenigk, K. F., and K.F.Jensen. "Low Pressure CVD of Silicon Nitride." *J. Electrochem. Soc.* 134 (July 1987): 1777-1785

34. Zhang, S. L., J. T. Wang, W. Kaplan, and M. Ostling. "Silicon Nitride Films Deposited from SiH_2Cl_2-NH_3 by Low Pressure Chemical Vapor Deposition: Kinetics, Thermodynamics, Composition and Structure." *Thin Solid Film.* 213 (1992): 182-191

35. Kern, W., and R. S. Rosler. "Advances in Deposition Processes for Passivation Films." *J. Vac. Sci. and Technol.* 14(1977): 1082

36. Claasen, W. A.P. *et al.*. "Influence of Deposition Temperature, Gas Pressure, Gas Phase Composition, and RF Freq. on Composition and Mech. Stress of Plasma SiN Layers." *J. Electrochem. Soc.* 132 (April 1985): 893

37. Bohn, P. W., and R. C. Manz. "A Multiresponse Factorial Study of Reactor Parameters in PECVD Growth of Amorphous Silicon Nitride." *J. Electrochem. Soc.* 132 (Aug. 1985): 1981

38. Olin Hunt. *Material Safety Data Sheet. U. S. Patent, # 4877651.* (1989)

39. Ohring, M. *The Materials Science of Thin Films. Academic Press. San Diego, California, U. S. A.* (1992): 189

40. Grow, J. M., R. A. Levy, M. Bhaskaran, H. J. Boeglin, and R. Shalvoy. "Low Pressure Chemical Vapor Deposition of Silicon Carbide from Ditertiarybutylsilane." J. Electrochem. Soc. 140 (Oct. 1993): 3001-3007

41. Habraken, F. H. P. M., A. E. T. Kuiper, A. V. Oostrom, Y. Tamminga, and J. B. Theeten. "Characterization of Low-pressure Chemical Vapor Deposited and Thermally Grown Silicon Nitride Films." *J. Appl. Phys.* 53(1) (Jan. 1982): 404-415